Industrial Wastewater Treatment Using

A South African Natural Zeolite, Clinoptilolite

Selilo Bethuel Semosa

A dissertation submitted to the Faculty of Engineering at the University of the Witswatersrand, Johannesburg, in fulfillment of the requirements for the degree of Master of Science in Engineering

University of the Witwatersrand, Johannesburg

DECLARATION

I declare that this dissertation is my own unaided work. It is submitted in completion of the requirements for the degree of Master of Science in Engineering at the University of the Witwatersrand, Johannesburg. It has not been previously submitted for any other degree or examination at any other University.

_____

Selilo Bethuel Semosa

__26th __Day Of _October___2005

DEDICATION

To my mother, brothers, sisters and
my beloved daughter Mahlatse Mihlali.

ABSTRACT

Natural zeolites are finding applicability in a broad range of industrial processes. This study assesses the potential applications of a South African natural zeolite, *Clinoptilolite*, and develops a methodology to quickly screen and assess these applications. Zeolites are known to have ion exchange and adsorption properties. Wastewater treatment has been identified as a potentially important opportunity in South Africa, since South Africa - and particularly Gauteng - is a water scarce region.

The wastewater treatment industry in this region can be divided into two main categories of effluent: namely chemicals from coal and the metal recovery and finishing related to the mining industry. The focus of this work was to find a method to screen for potential uses of Clinoptilolite in these industries.

The major effluent treatment issue in respect of the effluents from coal-based processes was identified to be the removal of oxygenate organics that are highly soluble in water, such as ethanol and acetone. This problem cannot be solved using vapour-liquid equilibrium based processes due to high energy costs, and liquid-liquid equilibrium based processes inherently introduce new contaminants into the wastewater. We therefore screened the zeolite for application in the removal of soluble organics via adsorption.

The zeolite was found to be unsuitable for the adsorption of acetone and ethanol due to the preferential adsorption of water. As a result we tested the potential of the zeolite as a drying agent for ethanol and acetone. It was found that this zeolite could find application in the dehydration of ethanol, but not acetone.

In effluent from the mining and metals based industries, heavy metals frequently occur and are usually toxic, such as lead, zinc and nickel. Such contaminated water must be disposed of as toxic waste, and this is very costly. Thus being able to selectively remove these metals allows for the possible recovery and recycling of a potentially valuable metal. If no application can be found for the recovered metal, the loaded zeolite would

need to be disposed of as toxic waste, but the volume of this waste is significantly smaller than that of the original effluent due to the concentration effect of ion exchange processes.

All of the metals were ion exchanged onto the zeolite successfully. The zeolite exhibited exceptional selectivity for the removal of lead, and reduced the concentration of lead in the water to levels below detection by Atomic Adsorption. The selectivity for the uptake of the metals in decreasing order was lead, zinc and lastly nickel. Therefore, provided the zeolite can be regenerated, it could be used for effluent treatment in mining activities that have traces of lead in the ore body, such as zinc and silver deposits, and in the battery industry.

As a result of the work presented in this dissertation, a further project was undertaken to investigate the regeneration of the zeolite. Preliminary findings indicate that although it can be regenerated, the zeolite capacity decreases with each successive regeneration cycle. More work is required on regeneration to improve the lifespan of the zeolite.

ACKNOWLEDGEMENTS

I hereby wish to express my heartfelt gratitude to the many people whose support has made the completion of this work possible. Special mention goes to the following people:

I am most grateful to the man upstairs, the Almighty God, who has blessed me in more ways than I can count.

A special thanks to Dr Linda Jewell, for her understanding, advice and intellectual criticism during the course of this study. I must acknowledge her patience and moral encouragement, her editorial suggestions and her interest in the progress of this investigation.

Sincere appreciation is also expressed to Professors Hilderbrant and Glasser for their advice and brilliant suggestions during the course of this study.

To my colleagues in COMPS, Tumi, Khumalo, Geoffrey, and Simon Holland for showing interest in the completion of this work.

Thanks are expressed to Basil and the Wits Chemistry Department for their technical support.

To Rob Douglas for giving me time from work to complete my experimental studies.

Finally, I am very grateful to my friend, Simon Baloyi. You are indeed the Rock on which trust, courage and dreams can be built. Without him the realisation of this dissertation would probably not have been possible. Thanks for showing a deep interest in the completion of this work.

CONTENTS

LIST OF FIGURES

LIST OF TABLES

NOMENCLATURE

Å	Angstrom
TCD	Thermal conductivity detector
OD	Outside Diameter
GC	Gas chromatography
kPa	Pressure in Kilo pascals
G	Grams
ppm	Parts per million
AA	Atomic Absorption Spectroscopy
KA	Response factor of component A
KB	Response factor of component B
AreaA	Peak area of component A
AreaB	Peak area of component B
N	Number of sample injection
$\mathbf{R_i}$	Individual predicted mass fraction
R	Mean of the predicted mass fraction

Chapter 1 Introduction

1.1 General Introduction

The fate of trace elements and organic molecules in industrial and natural waters is of growing concern to the world population. Rapid industrialisation during the past century has led to the dissemination of a wide variety of pollutants, including toxic elements into the environment. Chemical contaminants at low concentrations are difficult to remove from water.

Treatment processes for contaminated waste streams include chemical precipitation, membrane filtration, ion exchange and adsorption. Cost effective alternative sorbents for treatment of contaminated waste streams are needed. Although there is increasingly strict legislation regarding permissible effluents, due to economic pressure companies are unable to spend vast sums of money on environmental clean-up operations. As a result, inexpensive solutions are sought. Natural materials that are available in large quantities, or certain waste products from industrial and agricultural operations, may have potential for use as inexpensive sorbents.

Scattered research has already been conducted on a wide variety of sorbents, and natural zeolites are reported to be a low-cost adsorbent (Bailey et al, 1999). The adsorption properties of zeolites result from their ion exchange and molecular sieve capabilities. Clinoptilolite is one of more than 40 naturally occurring zeolite species and 150 synthetic zeolites (Bailey et al, 1999; Tihmillioglu and Ulku, 1996). Due to abundance, it is readily available and inexpensive.

1.2 Aims and Objectives

Since the composition and quality of a natural zeolite depends on its origin, it is necessary to assess the potential of South African Clinoptilolite as an adsorbent and ion exchanger independently. Wastewater treatment has been identified as a potentially important opportunity in South Africa, since South Africa - and particularly Gauteng - is known to be water scarce region.

The aim of this study is to find potential applications and to develop a methodology to quickly screen for a South African natural zeolite, Clinoptilolite, as an adsorbent for:

(a) Oxygenated organics which are highly soluble in ethanol and water, and which are present in effluents from coal based processes; and
(b) Lead, zinc and nickel since these metals frequently occur in effluent from the mining and metals based industries and are usually toxic.

Chapter 2 Literature Review

2.1 Zeolites

A zeolite is a highly crystalline silica-alumina structure. The silicon and aluminium atoms are connected to one another by oxygen bridges arranged tetrahedrally around them. Due to the difference in valence between silicon and aluminium, wherever an aluminium atom occurs in the lattice there is an associated charge imbalance. The charge imbalance is satisfied by an extra-lattice counter ion. Since the lattice has a resultant negative charge, these counter ions are positive. The counter ions in the zeolite can be exchanged with ions in the liquid phase in the pores of the zeolite. A particular zeolite will exhibit different selectivities for different ions depending on the size and charge density of the ion. A particular zeolite structure may also have a range viable Si:Al ratios; the viability of a ratio would be determined by the stability of the structure.

Zeolites were first recognised by Swedish mineralogist Cronstedt (1756) as a new group of minerals of hydrated aluminosilicates of the alkali and alkaline earths with his discovery of stilbite. The minerals exhibited intumescence, which is the phenomenon of swelling up. Therefore he called the mineral a zeolite, which comes from the Greek words "Z$\in$0" meaning " to boil" and "$\lambda\theta$os" meaning "stone".

Zeolites may be represented by the empirical formula (Breck, 1974):

$$M_{2/n}O.Al_2O_3.xSiO_2.yH_2O$$

In this oxide formula, x is generally equal to or greater than 2 since AlO_4 tetrahedra are joined only to SiO_4 tetrahedra, n is the cation valency.

2.2 Zeolite Structures.

Zeolites are crystalline alumino-silicates with an infinitely extended open three-dimensional anionic network. The fundamental unit is a tetrahedral complex consisting of a small cation, such as Si^{4+}, in a tetrahedral coordination with four oxygens (Figure 2.1). The Al^{3+} ion commonly coordinates tetrahedrally as well as octahedrally with oxygen in silicates (Breck, 1974).

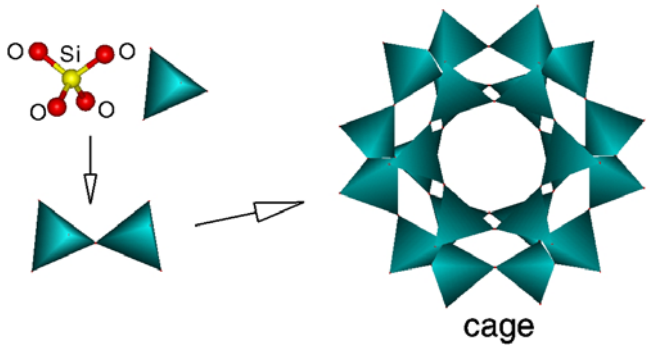

Figure 2.1 Representation of SiO_4 or AlO_4 Tetrahedron (Natural and Synthetic Zeolites, 1987).

Zeolite structures can be visualized by taking a neutral SiO_2 framework and isomorphously substituting AlO_2^- for SiO_2. The resulting structure then exhibits a net negative charge located on the framework aluminium. This negative charge is balanced by an alkaline or alkaline earth metal ion (cations) that resides in the interstices of the framework. Many of these cations are mobile and free for exchange. This ion exchange property accounts for the greatest volume use of zeolites (Marcus and Cornier, 1997).

There are about 40 natural zeolite structures that have been identified during the past 200 years; the most common are analcime, chabazite, Clinoptilolite, erionite, ferrierite, heulandite, laumontite, mordenite, and phillipsite. More than 150 zeolite structures that do not occur in nature have been synthesized and the most common are zeolites A, X, Y, and ZMS-5 (Virta, 2000). However, it is not the aim of this chapter to present an

exhaustive description of all structures so only the Clinoptilolite structure, which is the zeolite used in this project, will be described.

Clinoptilolite is very closely related to heulandite. It is considered to be a high-silica member of the heulandite group and crystallizes in the monoclinic system (Mumpton, 1960). Clinoptilolite, which means " *oblique feather stone*" in Greek, received its name because it was thought to be the monoclinic (or oblique inclined) phase of the mineral ptilolite, as in "*oblique ptilolite*" (Mumpton, 1978).

The ideal composition of Clinoptilolite is $(Na,K)_4Ca.Al_6\ Si_{30}O_{72}.24H_2O$. By definition, the Si:Al ratio of Clinoptilolite can vary between 4.0 and 5.25.

Clinoptilolite forms as a devitrification product (the conversion of glass to crystalline material) of volcanic glass in tuffs. Tuffs are consolidated pyroclastic rocks. The devitrification occurs when the glass is in contact with saline waters. Clinoptilolite is also found in the vesicles of volcanic rocks such as basalts, rhyolites and andesites. It forms as an alteration of phillipsite in deep-sea sediments and with borate minerals in playa lakes (Sheppard and Gude, 1968). Based on commonly observed assemblages, the following possible reactions for Clinoptilolite formation were suggested (Couture, 1977):

(a) Basaltic glass + silica (mainly biogenic) → Clinoptilolite

(b) Smectite + phillipsite + biogenic silica → Clinoptilolite + palygorskite

Clinoptilolite is one of more than 40 naturally occurring zeolite species and 150 synthetic zeolites (Tihmillioglu and Ulku, 1996). Large deposits of the mineral are known in Japan, Italy, Hungary, Bulgaria, Soviet Union, United States and South Africa. The zeolite used in this project is natural South African Clinoptilolite supplied by Pratley Perlite Mining Co. (Pty) Ltd. in South Africa. The walls of the channels of Clinoptilolite consist of 8- and 10-membered rings, with a pore size of 3.5-6Å. This particular Clinoptilolite has a Si:Al ratio of 3.85Å. The typical structure of Clinoptilolite is shown in Figure 2.2 and the

physical properties of South African Clinoptilolite are shown in Table 2.1 (Natural Zeolite Data Sheet).

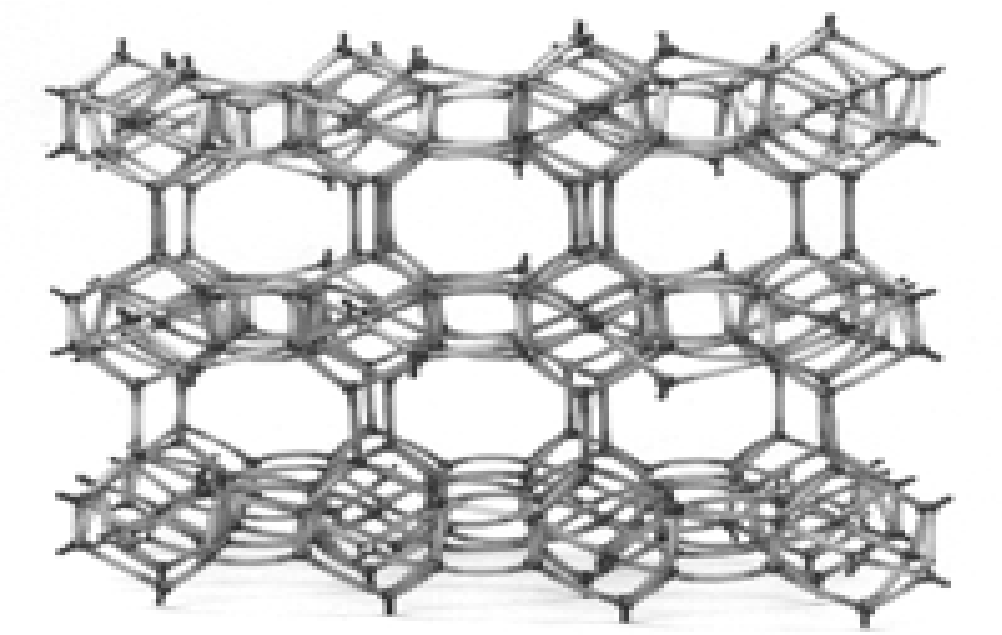

Figure 2.2 Typical Structure of Clinoptilolite (Natural and Synthetic Zeolites, 1987).

Table 2.1 Crystal Structure Data for Clinoptilolite (Pratley Natural Zeolite Data Sheet)

Structure Group: 7

Chemical Composition

Typical Oxide Formula: $(MgCaNa_2K_2)_{2.5}(AlO_2)_7\ (SiO_2)_{30}21H_2O$

Typical Unit Cell Contents: $CaNa_4.\ (AlO_2)_8.(SiO_2)_{30}.24H_2O$

Variations: Si/Al 3.85; water rich

Variety has 30 H_2O

Elemental Analysis:

Element	**Weight Percentage**	**Element**	**Percentage**
SiO_2	71.52	MnO	0.07
Al_2O_3	12.10	Cu	Trace
Na_2O	1.40	Co	Nil
K_2O	3.85	Pb	0.009
MgO	0.86	Ni	Trace
CaO	1.53	Cr	Trace
Fe_2O_3	1.21	Ba	Trace
TiO_2	0.13	Total water	7.30

Physical Properties (Pratley Natural Zeolite Data Sheet)

Main Phase:	80-85% Clinoptilolite [XRD, BET & Analysis)
Main impurities:	Paline Cristobalite, K-Feldspar & trace of sanidine
Refractive index:	1.484
Density or Specific gravity:	2.2g/cm3
Bulk Density of the ore:	1.92 g/cm3
Packing Density:	0.99 kg/m3
Thermal Stability:	It can be heated to over 700^0C before the aluminosilicate framework collapses
Acid and Alkaline Stability:	Stable from pH 3 to pH 12
Colour:	Reflection white: 80% [MgO=85%]
Hardness:	Hardness is 3.5-4.0 MOH
Pore Size:	3.5-6 angstroms [3.5Å]
Pore Volume:	Approximately 5-10%, the bulk density of the rock as determined by immersion in mercury is 1.92 g/ml^3

2.3 Ion Exchange and Adsorption Properties of Clinoptilolite.

As mentioned earlier Clinoptilolite is known for its ion exchange and adsorption properties (Bailey et al, 1999; Tihmillioglu and Ulku, 1996). These properties will be discussed in detail in the section that follows:

2.3.1 Ion Exchange Properties

Natural zeolites, and Clinoptilolite in particular, manifest characteristics that are typical of ion exchangers. The isomorphous replacement of silicon atoms by aluminum within a

zeolite lattice gives rise to a negative charge on the framework. Although this negative charge is partially delocalised over the whole framework, 'pockets' of localised charge are still found throughout the lattice (Bailey et al, 1999; Tihmillioglu and Ulku, 1996).

A more obvious consequence of the presence of this negative charge on the lattice arises from the need for electroneutrality to be preserved within the zeolite. The sizes of channels and cages within the zeolite are such that the silicate layers or sheets are able to move apart, permitting occlusion of water molecules; consequently exchange between the cations originally present between the layers and (different) cations in the external solution is possible.

The cation exchange behavior of zeolites depends upon:

1) the nature of the cation species, the cation size (both anhydrous and hydrated) and the cation charge;
2) the temperature;
3) the concentration of the cation species in solution;
4) the anion species associated with the cation in solution;
5) the solvent (most exchange has been carried out in aqueous solutions, although some work has been done in organic solvents) (Bailey et al, 1999; Tihmillioglu and Ulku, 1996); and
6) the structural characteristics of the particular zeolite.

Cation selectivities in zeolites do not follow the typical rules that are evidenced by other inorganic and organic exchangers. Zeolite structures have unique features that lead to unusual types of cation selectivity and sieving. The structural analyses of zeolites form a basis for interpreting the variable cation exchange behaviour of zeolites (Breck, 1974; Townsend, 1984).

Even though zeolites possess interesting ion exchange properties, applications of these materials as ion exchangers are not widespread (Townsend, 1984). There are two main

reasons: First, many zeolites are relatively unstable even in mildly acidic solutions (such as pH 4 to 5). To attain a high resistance to acid attack, a material with a high silicon: aluminium ratio is needed (for example mordenite or Clinoptilolite). The higher the value of this ratio, the lower the exchange capacity of the zeolite. Secondly, there are problems in obtaining a satisfactory rate of exchange for column operation. While the rate at which a given ion exchanges into, for example, discrete crystallites of zeolite A frequently bears comparison with exchange for the same ion into a typical macroreticular resin at ambient temperature, operating a column using a bed of zeolite crystallites (size typically 8μm) is impractical. In order to obtain an acceptable throughput rate, it is necessary to pelletise the zeolite. This results in a drop in the exchange rate to a value which is often far below that found for a macroreticular resin of comparable bead size.

Despite these drawbacks, zeolites have lately found a number of specialised, but nevertheless important, direct applications as ion exchange media (Townsend, 1984). Zeolites have found practical application as ion exchangers only in those specialised areas in the market where resins are unsuitable. Where resins or zeolites are interchangeable, the resins remain the preferred materials. “Therefore it is instructive to start making comparison of the general properties of resins and zeolites; then, the reasons why zeolites have found these rather specialised ‘niches’ becomes apparent”(Townsend, 1984). Comparison of the general properties between zeolites and resins are shown in Table 2.2.

Table 2.2 Comparison of Resins and Zeolites

Property	**Resin**	**Zeolite**
Chemical nature	Organic co-polymer	Aluminosilicate crystals
Structure	Amorphous	Crystalline
Porosity	Disperse, about 10nm	Specific, less than 1nm
Particle size	Variable, up to several mm	0.1-50μm
Ion sitings	Non-specific	Clearly defined sets of sites
Thermal stability	Low	Usually high
Solution stability	High	Usually low
Radiation stability	Usually low	High
Mechanical strength	Variable	Usually high
Attrition resistance	High	Variable
Cost	High	Usually low

There are four main areas where zeolites are directly applied as ion exchangers. These are, in order of decreasing importance: in detergents; in ammonia/ammonium removal from freshwater effluent; in radio-isotope removal from spent pile effluent; and in agriculture (Townsend, 1984). Zeolites are used in the removal of ammonia and ammonium ions from freshwater effluent, especially Clinoptilolite (Hein et al, 1999).

2.3.2 Adsorption Properties

The ability to preferentially adsorb certain molecules, while excluding others, has opened up a wide range of molecular sieving applications. This ability to sorb considerable volumes of sorbate molecules, in place of the zeolitic water present in the crystals on formation, was demonstrated by early studies (Rees and Williams, 1964). The molecular volume and shape of the sorbate molecules was found to have an influence upon the amounts, which could be taken up by the zeolite.

Adsorption properties of a particular zeolite are determined by two different properties of the zeolite: the pore size and the affinity of the zeolite for the molecules to be adsorbed relative to the molecules that are to be rejected. The pore size distribution can be used to discriminate between small molecules that are able to move into the pores and larger molecules that are too big to fit.

The ability to modify slightly the channel sizes and the nature of the exposed surface in zeolites is of great importance (Whan, 1981). Such 'fine tuning' of the adsorptive properties of zeolites is also of considerable significance when zeolites are employed as catalyst supports. The adsorption properties of zeolites can be modified in one or more of the following ways:

1) The unit cell dimensions of zeolites vary with silicon to aluminium ratio. For example, in the case of faujasite there is a linear dependence of the size of the cubic unit cell from 24.60 to 24.95Å as the Si-Al ratio changes from 3.0 to 1.18 (Breck, 1974).
2) The incorporation of appropriate cations into zeolites by ion exchange can influence the size of the voids available for adsorption.
3) An increase in temperature enables larger molecules to enter zeolites, probably because of the increased amplitude of lattice vibrations.
4) The nature of the surface of the zeolite may be modified e.g. removal of aluminium. Highly silicious zeolites are inherently hydrophobic in character, whereas materials with a preponderance of surface hydroxyl groups tend to be hydrophilic.

2.3.3 Adsorption Isotherms

Two important physiochemical aspects for the evaluation of the adsorption process as a unit operation are the equilibria of the adsorption and the kinetics. Equilibrium studies give the capacity of the adsorbent (Muhammad et al, 1998). The equilibrium relationships between the adsorbent and the adsorbate are described by adsorption

isotherms, usually the quantity adsorbed and that remaining in solution at a fixed temperature at equilibrium. There are two types of commonly used adsorption isotherms, namely Langmuir adsorption and Freundlich adsorption isotherms.

2.3.3.1 Langmuir Isotherm

The simplest expression of equilibrium adsorption is the linear isotherm, which is valid for dissolved species that are present at concentrations less than one-half of their solubility at saturation. The Langmuir adsorption isotherm is often used for adsorption of a solute from a liquid solution.

In the Langmuir model adsorption increases linearly with increasing solute concentration at low concentration values and approaches a constant value at high concentrations. The adsorbed concentration approaches a constant value because there are a limited number of adsorption sites in the adsorbent.

The Langmuir adsorption isotherm is perhaps the best known of all isotherms describing adsorption and is often expressed as (Casey, 1997):

$$Q_e = X_m K C_e/(1+ K C_e) \quad \text{.....(1)}$$

Where:

Q_e is the adsorption density at the equilibrium solute concentration C_e (mg of adsorbate per g of adsorbent)

C_e is the concentration of adsorbate in solution (mg/L)

X_m is the maximum adsorption capacity corresponding to the monolayer coverage (mg of solute adsorbed per g of adsorbent)

K is the Langmuir constant related to energy of adsorption.

2.3.3.2 Freundlich Isotherm

Freundlich isotherm was developed before the Langmuir isotherm and describes adsorption in which the number of adsorption sites is large relative to the number of contaminant molecules. The Freundlich adsorption isotherm is often expressed as (Casey, 1997):

$$Q_e = K_f C_e^{1/n} \quad \ldots\ldots\ldots\ldots\ldots\ldots\ldots\ldots\ldots\ldots\ldots\ldots\ldots\ldots\ldots (2)$$

Where:

Q_e is the adsorption density at the equilibrium solute concentration C_e (mg of adsorbate per g of adsorbent)

C_e is the concentration of adsorbate in solution (mg/L)

K_f and n are the empirical constants dependent on several environmental factors and n is greater than one

This equation is conveniently used in the linear form by taking the logarithms of both sides as:

$$\ln Q_e = \ln K_f + 1/n \ln C_e \quad \ldots\ldots\ldots\ldots\ldots\ldots\ldots\ldots\ldots\ldots\ldots\ldots\ldots (3)$$

2.4 Uses of Clinoptilolite

2.4.1 Ion Exchange Application of Clinoptilolite.

Clinoptilolite is generally inferior to resins or synthetic zeolites for industrial applications, due to reasons shown in Table 2 and their inability to be regenerated. However, due to costs there may be some reasons to use Clinoptilolite rather than resins

2.4.1.1 Application in the Nuclear Industry

The ion-exchange properties of Clinoptilolite have been investigated more intensively than those of any other natural zeolite, primarily because of its abilities to scavenge Cs^{137} from radioactive solutions and ammonium ions from municipal wastewater streams. In an early study of Clinoptilolite, Ames (1960) used minerals from the Hector deposit in the United States to selectively remove Cs^{137} and Sr^{90} from the low level radioactive water created by nuclear reactors. Mumpton (1978) has provided a detailed description of past and present uses of Clinoptilolite in the USA. Included among these uses are:

a) removal of Cs^{137} from high radioactive waste:
b) decontamination of low and medium level wastes; and
c) fixation of fission products into zeolites prior to long term storage.

The early success of Clinoptilolite for the removal of Cs and Sr in the United States nuclear industry was not reflected by worldwide use due to lack of general availability, and variability of composition of zeolite from one deposit to another. After the pioneering work of Ames (1960), several similar processes were developed, including one using chabazite to recover Cs^{137} from low level waste.

The availability of Clinoptilolite of uniform purity and composition (for example, from the Itaya mine in Japan and from certain Nevada deposits) has increased its current use in 'radwaste' treatment. In the UK, it is used to treat pond waters; in British Nuclear Fuels (BNF) and central Electricity Generating Board installations, its use is becoming standard practice (Dyer, 1984).

Work in progress seeks to extend the use of natural zeolites including Clinoptilolite to contain other radioisotopes present in nuclear wastewaters and secondary water circuits. Zeolites used in this area take advantage of their known resistance to radiation, in contrast to resin ion-exchangers, which lose capacity and selectivity under irradiation. Several studies show that zeolite/cement composites can withstand leaching by seawater

well. Thus these can be used for sea-dumping of low-level radioactive wastes (Mikhail, 1981).

Use of natural zeolites such as Clinoptilolite to treat "radwaste' does require detailed knowledge of their ion-exchange selectivities which vary with composition, that is, with geologic origin (Mikhail, 1981).

2.4.1.2 Ammonium Ion Removal from Waste Streams

In the last 20 years, the possible removal of ammonia from water containing alkaline earth salts and alkali salts by using Clinoptilolite has been the subject of laboratory investigations (Hein et al, 1999). It has also been applied industrially to some extent in connections with municipal wastewater treatment.

The early work of Ames (1960) demonstrated that Clinoptilolite had high selectivity towards ammonium ions and so could be used to treat sewage and agricultural effluents (Dyer, 1984). Clinoptilolite is highly ammonium-ion selective due to the size and charge of the hydrated cation and specific crystal structure and distribution of the exchange sites in the zeolite.

In the 1950s, Ames (1960) determined the ion selectivity series for Clinoptilolite as:

$$Cs^{+} > Rb^{+} > K^{+} > NH_4^{+} > Ba^{+} > Sr^{2+} > Na^{+} > Ca^{2+} > Fe^{3+} > Al^{3+} > Mg^{2+} > Li^{+}$$

Those cations that are more amenable to selection by Clinoptilolite are not commonly found in sewage streams, except for potassium. Clinoptilolite unusual selectivity for NH_4^{+} ions is caused by structurally related ion sieve properties found to differing degrees in many zeolites (Ames, 1960). Steric reasons determine the selective absorption of ammonium in the presence of bivalent cations, due to a molecular sieve effect because of different ionic radii (known as kinetic radii) (Dyer, 1984).

Koon and Kaufman (1974) reported that ammonium exchange capacity may be estimated from the cationic strength of the domestic wastewater and was observed to decrease sharply with increasing cationic concentration. They have also shown that the extent of ion sieving depends on:

a) the size of openings into the ion cages contained in the 3-D lattice structure; and
b) the energy or strength of bonding between the water and zeolite framework.

Choe et al (1999) undertook laboratory experimental studies to investigate removal of ammonium ions in bi-solute systems with either sodium or potassium ions. They found that ammonium exchange capacity in bi-solute system with sodium ions or potassium ions was reduced due to the competition with coexisting ions. Potassium ions reduce the exchange capacity more than sodium. This is agreement with the findings of laboratory studies carried out by Cooney et al (1999).

2.4.1.3 Transition Metal Ions Removal from Waste Streams.

Based on the pioneering work done by Chelishchev et al (1973), Clinoptilolite was found to be a useful ion-exchanger for Pb, Cu, Cd, Zn and Co in the final polishing step of the tertiary treatment of industrial wastewaters. Subsequently, research has been conducted in the United States showing the effectiveness of Clinoptilolite; Clinoptilolite from Bunker Hill, ID, Superfund site adsorbed large amounts of Pb even when competing ions were present (Bailey et al, 1999).

2.4.1.3.1 Lead Removal from Water

A study by Leppert (1990) reported that zeolites, Clinoptilolite in particular, demonstrate strong affinity for Pb and other heavy metals. Leppert's study reported that the overall ion exhange capacity for zeolites varies for different species, but tends to be around 1.5meq/g (155.4mg/g zeolite). An investigation was done on the leachibility of Pb from CRRs (Clinoptilolite-Rich Rocks) showing that CRRs could possibly be used for Pb removal

from wastewater and subsequently disposed of as non-hazardous waste. A preliminary report by Desborough (1995) stated that CRRs have preferential affinity for Pb over the other cations.

2.4.1.3.2 Selectivity Series of Heavy Metals Ion

In addition to high selectivity for Pb, Clinoptilolite has received extensive attention due to its good selectivities for certain heavy metals ions such as Zn^{2+}, Cd^{2+}, Ni^{2+}, Fe^{2+} and Mn^{2+} (Ouki and Kavannagh, 1999). The two authors studied selectivity of Clinoptilolite and found it to be highly selective for lead, copper and cadmium. Its selectivity sequence is as follows:

$$Pb > Cu > Cd > Zn > Cr > Co > Ni$$

2.4.2 Adsorptive Application of Clinoptilolite.

2.4.2.1 Drying Agent and Related Uses

Clinoptilolite acts as a suitable drying agent for both liquids and gases. There are several reports of Clinoptilolite being used as a drying agent for organic liquids such as transformer oil, xylene and freons (Tsitsishvilli and Pavliashvilli, 1980). Acid modified Clinoptilolite has been used to remove organic sulphur compounds from petroleum products (kerosene is 77-86 per cent desulphurised). The Hungarians market a Clinoptilolite tuff as 'Ersorb' for drying air, natural gas and carbon dioxide. The same product dried methanol, propan-2-ol, toluene and a petroleum feedstock to less than 1ppm of water. It was also used to fill drying cartridges in compression refrigerators.

Tihmillioglu and Ulku (1996) undertook a laboratory investigation of the use of Clinoptilolite as a potential dehydrating agent of ethanol. The study was motivated by the ethanol dehydrating ability of synthetic zeolites (zeolites 3A and 4A), and natural zeolite phillipsite (Teo and Ruthven, 1985; Colella et al, 1994). It was reported from the

investigation that Clinoptilolite seems to have a promising future as a dehydrating agent, but further work is required to upgrade the mineral before it can be used for commercial application.

On the other hand, hydrophobic zeolites were proposed as a selective adsorbent for removing organic molecules from aqueous solution (Whan, 1981). Suggested uses include decaffination of coffee, the manufacture of non-intoxicating beers by the selective removal of ethanol and removal of toxic materials from the blood.

2.4.3 Other Applications

Clinoptilolite has been used as paper filler, building material and aggregate in cement (Mumpton, 1978); in chromatography (Tsitsishvilli et al, 1980); and in agriculture as an animal feed additive and as a fertilizer. Potential uses include the harnessing of solar energy, use in zeolite synthesis and use in removal of toxic metals from solutions.

2.4.4 Concluding Remarks

Clinoptilolite is receiving extensive attention in the removal of heavy metals ions and ammonium ions from wastewater and removal of water from organic molecules. However, it is also noted from the literature that Clinoptilolite is a good adsorbent of lead and ammonium ions from all wastewater. It may be useful for the removal of organic pollutants from wastewater. It is noted from the literature that the adsorbent capacity of Clinoptilolite depends on its origins.

Thus from the literature we may conclude that the possible uses of the South African natural zeolite, Clinoptilolite, in the South African industrial context may include:

1) removal of soluble oxygenated organics from effluent streams; and
2) removal of toxic heavy metals ions from effluents from mining and metals based industries.

Chapter 3 Experimental Apparatus and Methods

3.1 Introduction

This chapter describes experimental work done in screening for possible removal of organic molecules and heavy metal ions from water by means of adsorption on Clinoptilolite. Since this is a screening exercise, quick, simple experiments are used; in this case batch experiments under ambient conditions. In this way, information on the adsorption of organic or heavy metals is obtained fairly quickly and simply.

The zeolite used in this experimental work is a natural South African Clinoptilolite supplied by Pratley Perlite Manufacturing and Engineering (Pty) Ltd in South Africa. The average size of the pores ranges between 3.5 and 6 Å, and the average particle size of the zeolite is between 2 and 3mm. This Clinoptilolite has the following chemical formula:

$$(MgCaNa_2K_2)_{2.5}(AlO_2)_7\,(SiO_2)_{30}21H_2O$$

3.2 Experimental Apparatus

3.2.1 Wrist-Action Shaker Machine

A wrist-action shaker machine (Figure 3.1) is used in the batch experiments to get good mixing between the liquid and zeolite particles, which tend to lie at the bottom of the flasks. The shaker is set at a constant speed so that all the results are comparable.

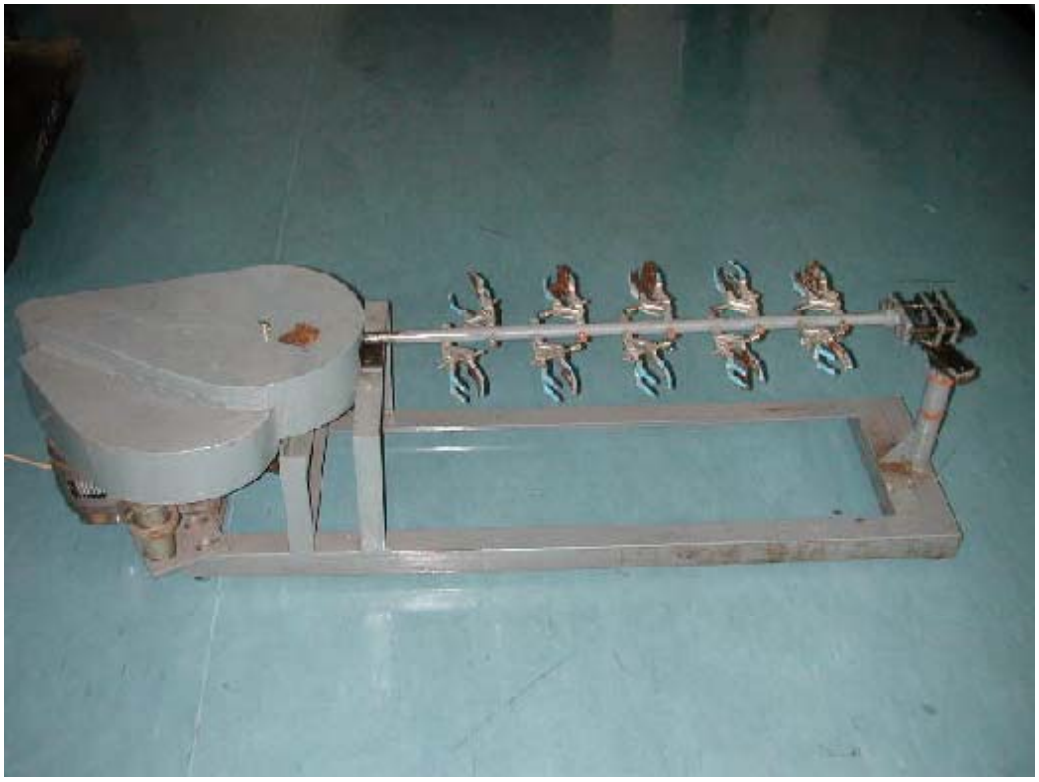

Figure 3 .1 Wrist-Action Shaker Machine

3.2.2 Gas Chromatography

Gas chromatography (Figure 3.2) was used to analyse the organic liquid sample compositions. A Porapak-Q packed column was chosen for this experimental work. The column has a diameter of 1/8 inch (OD) and a length of 3.5m. The thermal conductivity detector (TCD) is placed after the column. The detector responds to changes in thermal conductivity and the result is a chromatogram, a plot of the function of solute concentration versus time. Hydrogen was used as the carrier gas.

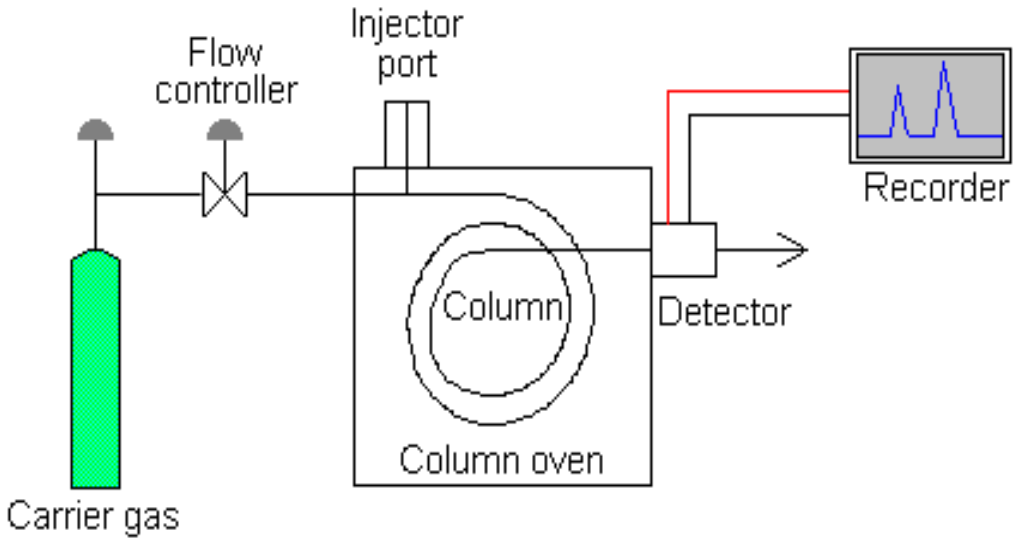

Figure 3.2 Gas Chromatography

3.2.3 Atomic Absorption Spectroscopy (AAS)

A SpectrAA 50/55 Atomic Absorption Spectrometer as shown in Figure 3.3 was used to analyse metal ion solutions. Instrument parameters such as lamp current, fuel, support gas and wavelength used for analysis of the metal ion of interest were as recommended in the SpectrAA 50/55 working manual.

Figure 3.3 SpectrAA 50/55 Atomic Absorption Spectroscopy (AAS)

3.3 Screening of Absorption of Organic Compounds

3.3.1 Chemicals Used

The chemicals screened in this section are ethanol and acetone. These oxygenated organics were chosen because they are the major effluent contaminant in the effluents from coal-based processes and they are highly soluble in water. It is known that as their hydrocarbon chain length increases, the solubility of a hydrocarbon decreases and hence ethanol and acetone were chosen because of their simple structure and size. They also mimic other organic molecules in the family of alcohols and ketones.

Analytical grade absolute alcohol (0.79g/L, minimum purity 99.995wt%) and analytical absolute acetone (0.73g/L, minimum purity 99.995wt%) obtained from Merck (Pty) Ltd. chemical company (Johannesburg, South Africa) were used for this experimental work.

3.3.2 Gas Chromatography Calibration

The process flow diagram for a gas chromatograph (GC) is shown in Fig 3.2. The chemical under investigation was first injected into the GC and the peak was observed. The retention time of each chemical injected was recorded. Various GC parameters such as flowrates, pressures and temperature were adjusted to obtain retention times that give sufficient separation within a reasonable time. Standard samples were prepared and injected into the operating GC. Peaks obtained from the GC were recorded using Hyperplot and PeakFit software and a response factor for each organic chemical under investigation was calculated and used throughout the experiments. The following is the detailed procedure carried out for calibrating the gas chromatograph.

3.3.3 Sample Preparation

Solutions of ethanol-water and acetone-water were prepared gravimetrically using a Precisa 180A balance accurate to 3 decimal places (i.e. 0.001g). The required mass of

organic liquid was added to a vial containing de-ionised water to give the desired concentration. Solutions were kept in a refrigerator to avoid vaporisation of the volatile component.

3.3.4 Sample Volume

For optimum column efficiency, the sample injected must not be too large, and must be introduced onto the column as a "plug" of vapour. Slow injection of large samples causes peak broadening and loss of resolution, thus the sample was injected quickly. The attenuation of the GC signal could be adjusted resulting in different sensitivities. For each attenuation, different sizes of samples measured in microliters were injected into the GC using a microsyringe.

The volume of sample to be injected was then selected based on attenuation and sensitivity, in order to obtain satisfactory results. This was done by plotting Volume against Area as shown in Figure 3.4 and Figure 3.5 for every attenuation and sensitivity. The higher attenuation the lower the sensitivity, so that it is desirable to operate at as low an attenuation as possible. Moreover, it was noted that as the attenuation is increased, a larger sample volume (as from 2 microliter) is required and hence high attenuation was not preferred. The linearity test was conducted to decide the region where the area output from the GC peaks in the linear region. This is critical for deciding the sample volume to inject since the amount of the component is directly proportional to the area under the GC peak only in this region. It was decided based on the linearity of the graphs shown in Figure 3.4 and 3.5 and the peak resolutions as shown in Figure 3.6 and Figure 3.7 to operate the gas chromatograph at an attenuation of 5 and to inject sample volume of 2 microliter. At higher attenuation, the large sample volume results in overlap between the peaks; making it difficult to integrate the peaks using Hyper plot. Sample volumes less than 2 microliter yielded smaller peaks that were also difficult to integrate using Hyper plot, due to background noise.

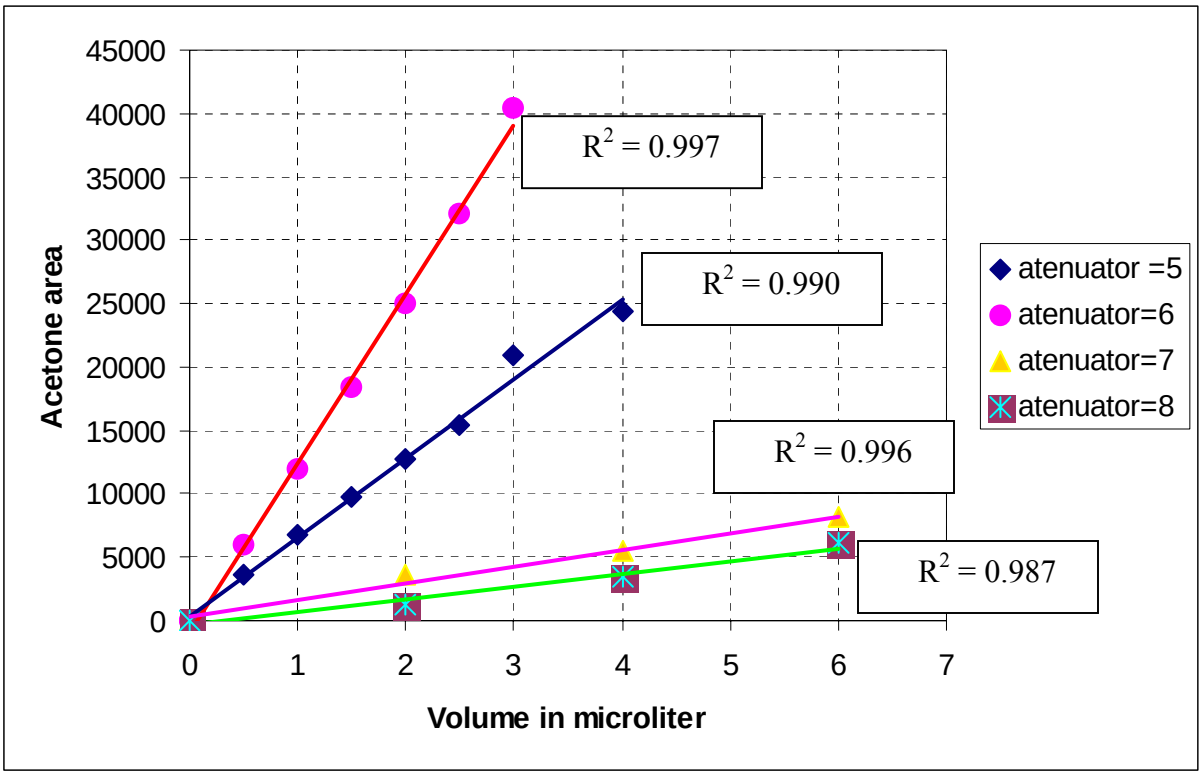

Figure 3.4 GC Linearity Curve (Volume vs Acetone Area)

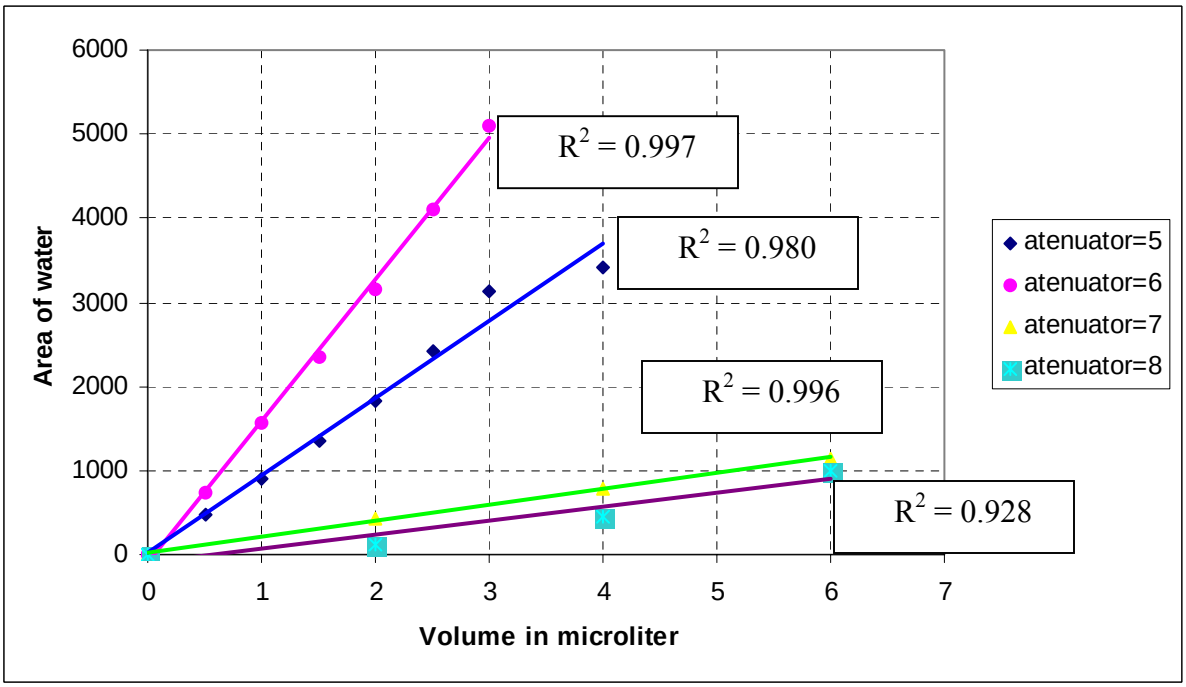

Figure 3.5 GC Linearity Curve (Volume vs Water Area)

3.3.5 GC Operating Conditions

The GC operating conditions were determined by considering the time it takes for all component peaks to appear (sample residence time), the extent of peak resolution and the shape of the peaks. Operating conditions were determined by changing column temperature and carrier gas flowrate until the peaks were well separated and could be accurately integrated using Hyperplot and Peakfit software.

3.3.5.1 Operating Temperatures

The injector temperature was set about 20^0C higher than the boiling point of the least volatile component of the sample. The column temperature was varied until good resolution of the peaks was observed. The column temperature was maintained at 180^0C, which is below the specified maximum temperature for the Porapak-Q column. The detector temperature was set to 30^0C above the column temperature. The operating temperatures are tabulated in Table 3.1.

Table 3.1 Operating Temperatures

Measurement	**Readings**
Injector Temperature	120^0C
Oven Temperature	180^0C
Detector Temperature	210^0C

3.3.5.2 Operating Pressures

The carrier gas flowrate was measured using a soap bubble meter and set by controlling the detector and reference flow control valves on the gas chromatograph. The carrier gas flow to the chromatograph is split to the detector line and the reference line. Both the

reference flowrate and column flowrate were set to be the same at 10 mL/min. The column was operated at the pressure of 200 kPa.

3.3.5.3 Column Conditioning

Since the stationary phase tends to decompose thermally to a very small extent, decomposition products were continuously removed by passing carrier gas through the column overnight at elevated temperature. The septum was replaced after every experiment to ensure that there was no leakage.

3.3.6 Methodology

It is important that the experimental technique used is accurate and errors are minimised prior to the commencement of the experiments. A program called Hyperplot was used to integrate the peaks from the GC traces. To obtain accurate results using Hyperplot, peak separation must be such that the detector response effectively returns to the base line before the next peak appears. This was achieved using the methodology described below.

3.3.6.1 Peak Identification and Evaluation

The GC Peaks were observed by adjusting GC parameters until sufficient separation was achieved within a reasonable time (refer to Figure 3.6 and Figure 3.7). Samples were injected into the GC operating at different column temperatures, starting from a high temperature and continuing to lower temperatures. The retention time of the water peak was observed to be about 60 seconds while the retention time of the other components varied with column operating temperature.

The following observations were made when injecting samples with a low concentration of organic molecules, as the GC is operated at high column temperatures, the water peak tail seems to overlap with the start of the peak of the organic component as shown in Figure 3.6. This was not acceptable because it introduced errors when integrating the

peaks using Hyperplot. The temperature was reduced until the peaks were sufficiently separated as shown in Figure 3.7. GC peaks of acetone and water at different column temperatures are shown in Appendix A1.

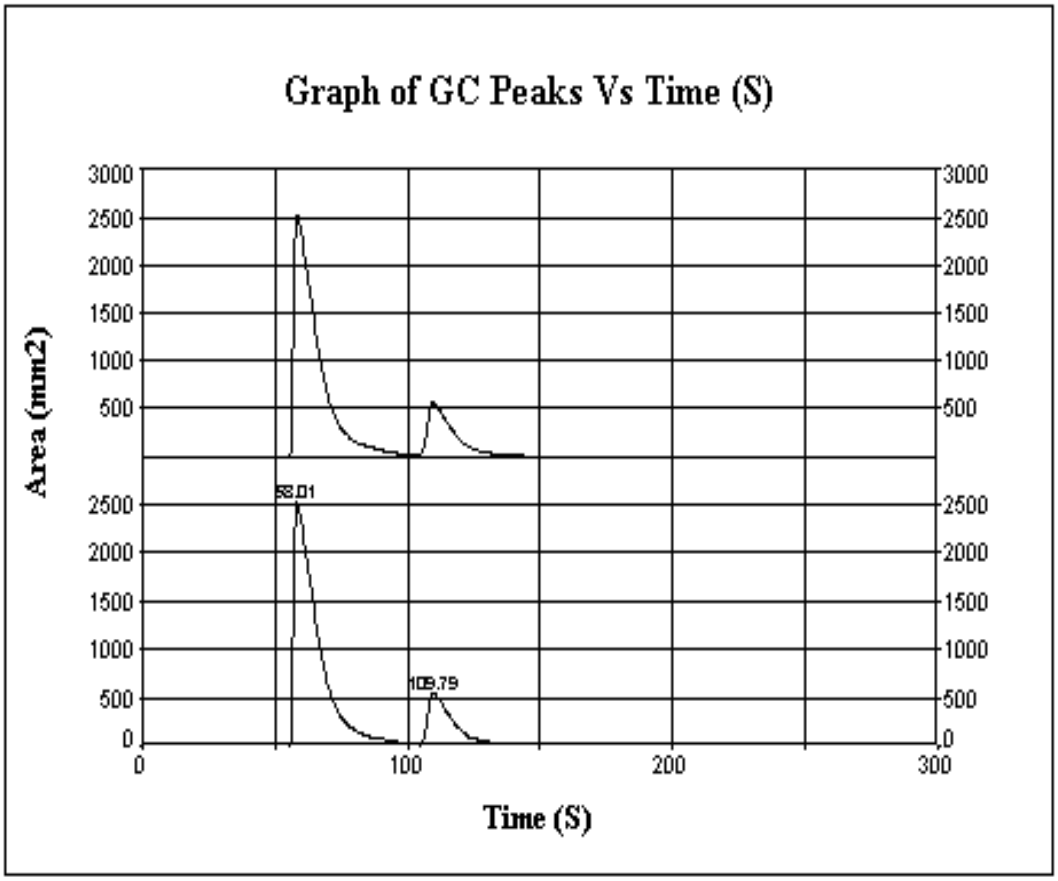

Figure 3.6: C Peaks of water and acetone at column temperature of 160^0C

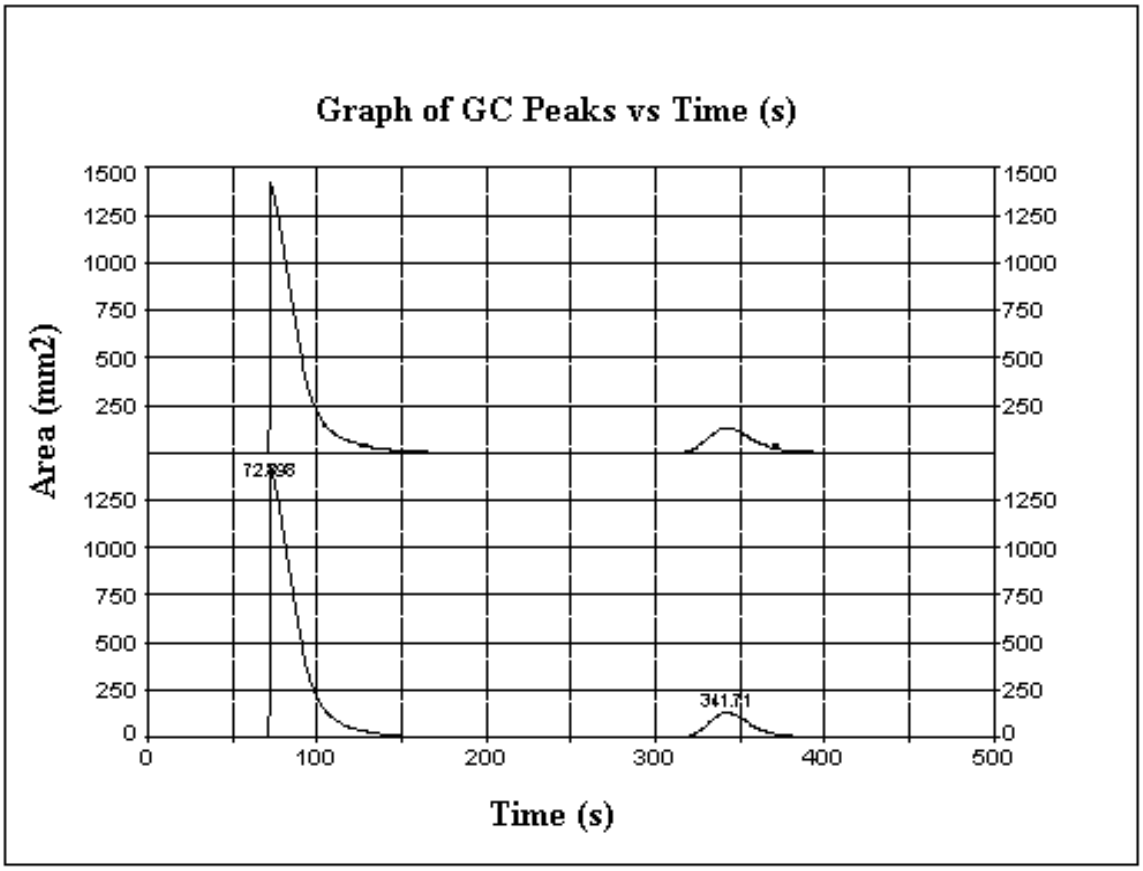

Figure 3.7: C Peaks of Water and Acetone at Column Temperature of 240^0C

3.3.6.2 Response Factors

The response factors were evaluated as follows: four samples with varying concentration ranging from high to low (as shown in Table 3.2 below) were injected into the calibrated GC.

Table 3.2: Acetone-Water Mixtures

Sample	Mass Of Water (g)	Mass Of Acetone (g)	Total Mass (g)	Mass Fraction Water	Mass Fraction Acetone
1	1.701	13.410	15.111	0.887	0.113
2	3.682	13.193	16.875	0.782	0.218
3	4.170	6.814	10.984	0.620	0.380
4	5.491	2.120	7.611	0.279	0.721

The peaks were recorded from the GC and the peak areas were obtained by integrating the peaks using Hyperplot. The area ratio of the two components is calculated and is shown in Table B2 (Appendix B). The concentration of the samples is calculated using the following equation for binary mixture as described by Dietz (1966).

$$\text{Mass fraction of A} = \frac{K_A * Peak\ AreaA}{K_A \times Peak\ AreaA + K_B * Peak\ AreaB} \quad \text{.....(4)}$$

Where K_A and K_B are the response factors of component A and B respectively. In this case A & B being acetone and water.

The response factor ratio of acetone to water (K_A/K_B) is calculated to be 1.217 with a standard deviation of 0.080 as shown in Table B2, B3 and B4 (Appendix B). The response factor ratio obtained in the literature (Dietz, 1966) for the two components is 1.236. The same procedure is used for obtaining the ethanol and water response ratio. The response factor ratio of ethanol to water is calculated in Table B5, B6, B7 and B8 in

Appendix B to be 1.140 with a standard deviation of 0.071, which also differs slightly from the literature (Dietz, 1966) value of 1.164. It can be concluded that the response factors obtained in this work are acceptable as there is no significant difference between the experimental and literature values, and the standard deviation between the experimental and measured values is small.

3.3.6.3 Reproducibility on Accuracy of GC Results

As has already been explained, the experimental work is done for screening purposes. The approach used to estimate the experimental errors is mainly on the reproducibility of the experimental results. A standard solution is prepared and injected five times into the calibrated GC. The GC peaks were integrated to obtain peak areas. The mass percentage is calculated using equation (4). The error calculated in this work is therefore the error in the reproducibility of the results. The reproducibility error in this work is defined as the standard deviation of individual predicted mass fraction from the mean, equation 5. The mean being the average of the individual predicted mass fractions.

$$\text{Standard deviation} = \sqrt{\left(\frac{1}{N-1}\sum(R_i - \overline{R})^2\right)} \quad \ldots\ldots\ldots\ldots\ldots\ldots\ldots\ldots(5)$$

Where R_i is the individual predicted mass fraction and $\overline{R}$ is the mean of the predicted mass fractions and N being the number of injections.

a) Ethanol-Water Mixture GC Experimental Errors

Ethanol-water mixtures of 86 mass% and 7.5 mass% were prepared and each injected five times into the GC. The mass fraction is calculated for every injection. The standard deviation from the mean of the predicted mass fractions is calculated using equation (5) and is presented in Table C1 and C2 (Appendix C). For 86 mass% ethanol solution, the mean is calculated to be 0.868 with a standard deviation 0.0014 and for 7.5 mass% ethanol, the mean is 0.0079 with a standard deviation of 0.0032.

b) Acetone-Water Mixture GC Experimental Errors

Acetone-water mixtures of 89.5 mass% and 8.7 mass% were prepared and each injected five times into the GC. The mass fraction is calculated for every injection. The standard deviation from the mean of the predicted mass fractions is calculated using equation (5) and Table C3 and C4 (Appendix C). For 89.5 mass% acetone, the mean is calculated to be 0.895 with a standard deviation of 0.0029 and for 8.7 mass% acetone, the mean is 0.0864 with a standard deviation of 0.0009.

3.3.7 Experimental Procedure for Screening of Organic Liquids

1) Clinoptilolite was first washed thoroughly (about 10 times in a 5L conical flask) with de-ionised water.
2) The washed zeolite was allowed to dry at room temperature for a period of 24hrs before use.
3) An organic solution of known concentration was then prepared by weighing a known mass of de-ionised water and pure organic liquid into a 250mL glass beaker, using the Precisa 180A weighing balance.
4) 10, 20, 30, 50 g of the dried zeolite was weighed into conical flasks.
5) The solution was poured into the conical flasks containing 10, 20, 30, 50g of dried zeolite. Part of the solution was poured into a glass vial and analysed using gas chromatography.
6) The conical flasks were placed on a wrist-action shaker machine that was switched on simultaneously with the starting of a stopwatch.
7) 2mL Samples were then taken at 8 hourly intervals and the experiment was run for a period of 3 days to allow equilibration of the solution. The collected samples were stored in a refrigerator if not immediately injected into the GC to avoid vaporisation of the more volatile component.
8) The gas chromatograph was turned on and injector, column and detector temperature was allowed to stabilise.
9) Samples were injected into the gas chromatograph and a 5 1/4[11]disk was used to store the data.

10) Hyperplot was then used to integrate the peaks obtained from the gas chromatograph.

3.3.8 Screening of Adsorption of Metal Ions

3.3.8.1 Introduction

The objective of this section is to describe the experimental work done in screening for possible removal of metal ions from water using local Clinoptilolite. The exchange of the following metals ions was investigated: Ni^{2+}, Zn^{2+} and Pb^{2+}. These metals were chosen because of their abundance in South Africa and are mined and processed by the mining and metal-based industries. They are also used in various industrial applications. Nickel catalysts are widely used in petrochemical industry while zinc and lead are used in battery industries. These metals are easily washed into streams and ground water. They are toxic to biological life including the people who may have to drink water from the polluted rivers.

3.3.8.2 Chemicals Used

1000ppm Standard metal laboratory grade solutions of nickel, zinc and iron were obtained from Merck (Pty) Ltd. chemical company (Johannesburg, South Africa) and were diluted using de-ionised water to the required concentration in ppm. Care was taken to ensure that the solutions were not contaminated before use, since the purity of the reagents determines the accuracy of the results.

3.3.8.3 Calibration Procedure

3.3.8.3.1 Sample Preparation

Calibration samples with the following concentrations: 5, 10, 15, 20, 30, 40 and 50ppm were prepared for each metal ion. These standards were analysed and were found to be in

agreement with the calibration curves in the atomic absorption spectrometry-working manual. For zinc, however, the seven standards prepared were further diluted because the AA gave an error signal due to the high concentration at the selected wavelength.

The absorbance obtained from the AA was corrected by multiplying with a dilution factor. The nickel, zinc and lead calibration curve were plotted as shown in Figure 3.8, Figure 3.9 and Figure 3.10, respectively.

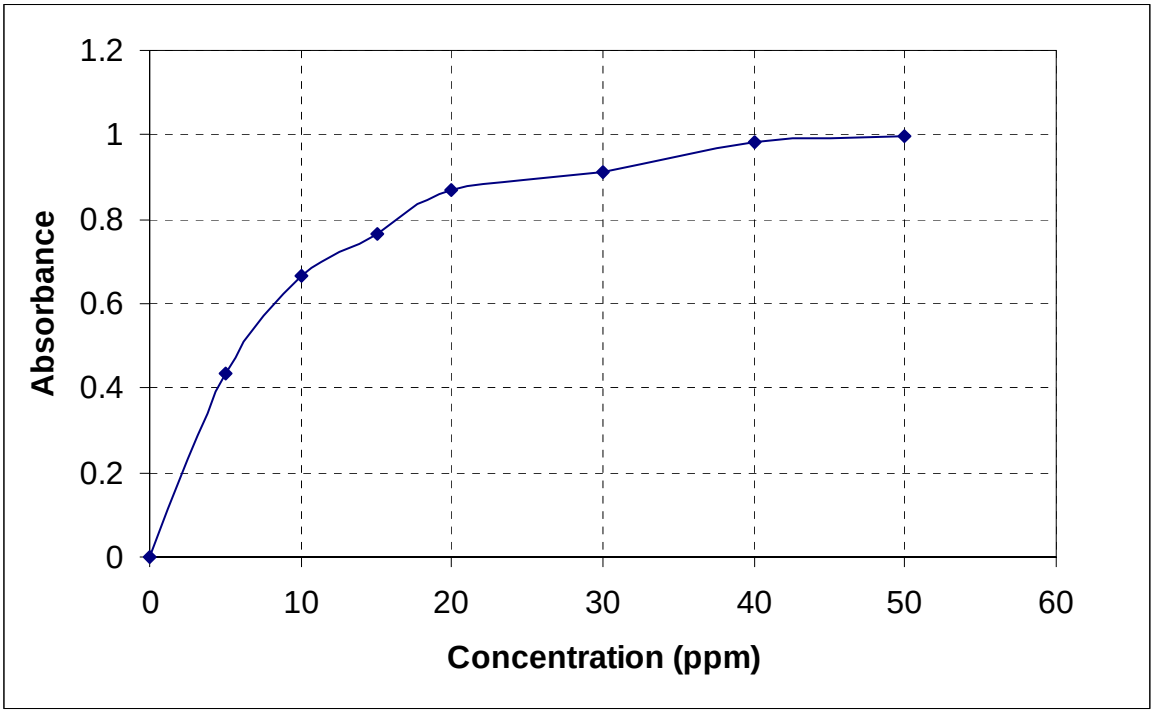

Figure 3.8 Calibration Curve for Nickel

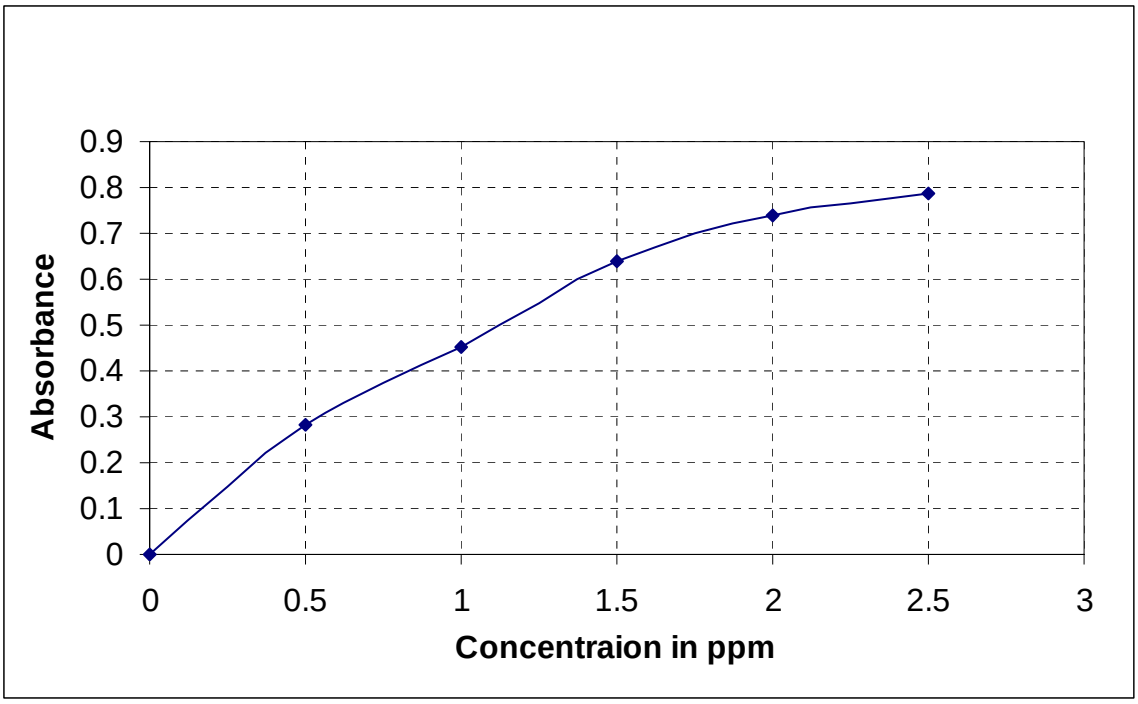

Figure 3.9 Calibration Curve for Zinc

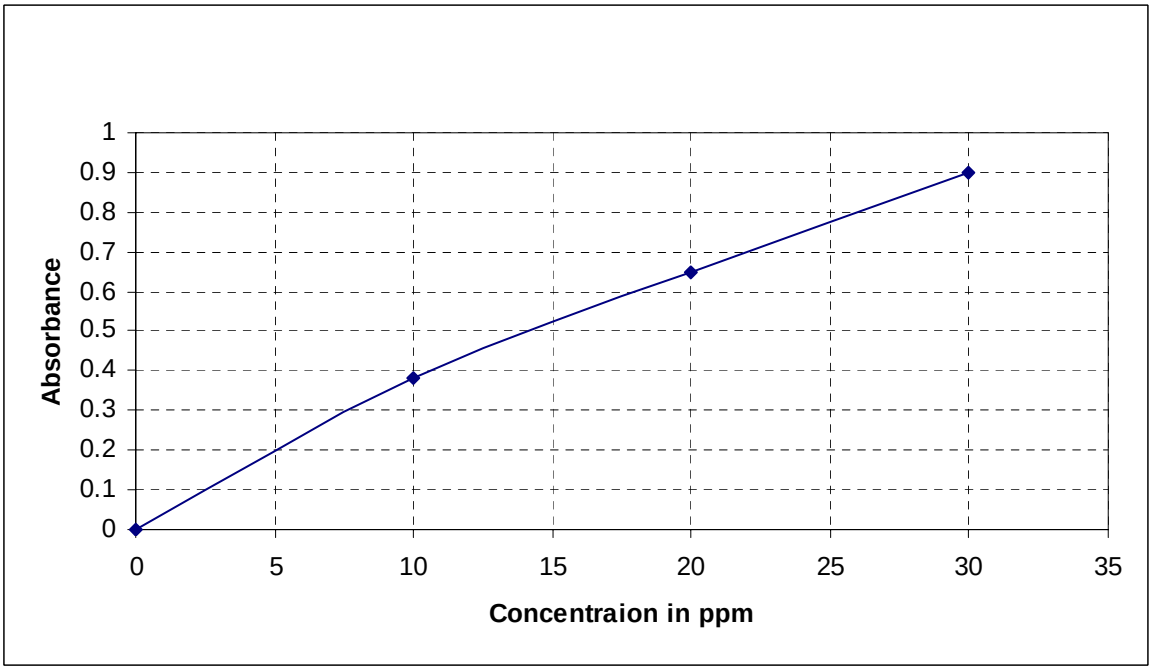

Figure 3.10 Calibration Curve for Lead

3.3.8.4 Operating Conditions and Procedure for the AA

The following procedure was used to ensure that accurate results were obtained. It was important for the operator to respond immediately to an error signal displayed by the machine, otherwise the results obtained would not be accurate.

- It was firstly ensured that the correct burner for a particular element under investigation was used and that the correct lamp was used. The machine was switched on and left for 10 minutes to stabilise and to perform its initialisation tests.

- The following parameters were loaded and saved after 10 minutes: element, method number, instrument mode, active lamp current, gas type, wavelength and slit width. It is important that the lamp is correctly positioned and the wavelength should be checked.

- The concentrations of the standard samples were entered. After entering the concentration values of standard samples, the lamp was left for 10 minutes for the signal to stabilise. The two knobs on the lamp were adjusted until the optimal signal was obtained.

- The gas flow was set so that the pressure recommended for a particular gas was used. The liquid trap was filled with water to about two-thirds. The flame was switched on and 50mL of water was sucked until it was apparent that the flame was stable. The drain tube was monitored to ensure that the water was drawn into the AA to ensure that the flame was stable. If there were no water droplets coming out of the drain tube, the machine was switched off and the liquid trap was washed to remove the deposit and to ensure that the tube was not blocked.

- The standard samples were checked to ensure that they were within the signal range. The smallest concentration gave at least 0.02 absorbance. The maximum standard sample concentration was checked to make sure that it was not out of signal range.

3.3.8.5 Experimental Procedure for Screening of Heavy Metals

1) Clinoptilolite was first washed thoroughly (about 10 times in 5L conical flask) with de-ionised water.
2) The washed zeolite was allowed to dry at room temperature for a period of 24hrs before use.
3) Metal ion solution of known concentration was then prepared by diluting the supplied 1000ppm standard solution using de-ionised water. The diluted solution was added into 250mL-glass beaker.
4) 10, 20, 30 and 50g of the dried zeolite was weighed into conical flasks.
5) The solution was poured into the conical flasks containing 10, 20, 30 and 50g of dried zeolite. The volume of solution used was 100mL.
6) The conical flask was placed on wrist-action shaker machine, which was switched on simultaneously with a stopwatch.
7) 2mL samples were then taken at 1 hour time intervals and the experiment was run for a period of 8 hours to allow for equilibration.
8) Before the atomic absorption was turned on, a pre-analysis checklist was carried out to ensure optimum operating conditions of the AAS.
9) The collected samples were analysed using optimum operating atomic absorption spectrometry.

Chapter 4 Results and Discussions

4.1 Introduction

This chapter reports the results and discussion of the experiments carried out in screening for possible removal of oxygenated organic molecules and metal ions from water. The experimental results obtained in this work are compared with related work as reported in the literature (Tihmillioglu and Ulku, 1996; Ouki et al, 1999; Bailey et al, 1999). What makes this work unique is that South African Clinoptilolite is used for evaluation.

4.2 Ethanol Adsorption Screening Results.

Tihmillioglu and Ulku (1996) carried out a study of the water-ethanol system, as discussed in Chapter 2, Section 2.4.2.1. The aim of their study was to investigate the possibility of ethanol dehydration using Clinoptilolite provided for their study by the American Colloid Company, and only a water-ethanol mixture with high concentration of ethanol was investigated. Furthermore, the preconditioning of the zeolite, Clinoptilolite, was not the same as in this work. The zeolite used in their investigation was preconditioned by thermal activation in a furnace at 300^0C. The zeolite used in this work was South African Clinoptilolite and was washed with de-ionised water and left to dry at room temperature for 24 hours. It was noted that after drying at 300^0C, when an aqueous solution was added to the zeolite, the adsorption was exothermic.

Due to concerns about the effect of this exotherm on the adsorption measurements, and the cost of drying raising questions about the use of dry zeolite in practical applications, it was decided to proceed with zeolite that had been dried under atmospheric conditions overnight.

This work considered both high and low concentrations of ethanol. The removal of low concentrations of ethanol from water was investigated using South African Clinoptilolite, which could be used as a low-cost adsorbent in environmental processes. The effect of

the amount of zeolite was also investigated. The experimental results are tabulated in Appendix D (table D1 and D2) and are plotted as shown in Figure 4.1 and 4.2. Figure 4.1 shows the changes in the ethanol mass fraction from an initial 6.7 mass% ethanol solution, for varying masses of zeolite.

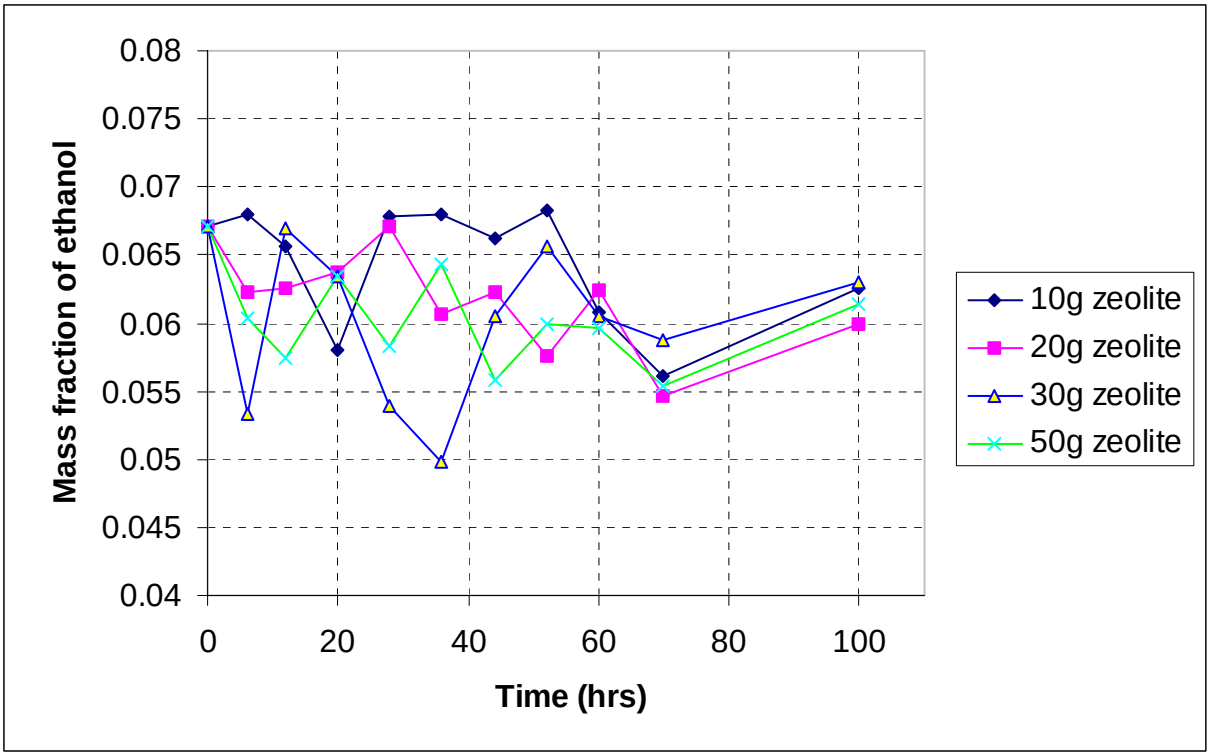

Figure 4.1 Changes in Ethanol Mass Fraction from an Initial Concentration of 6.7% Using Different Initial Masses of Zeolite

From the results shown in Figure 4.1, it is evident for the ethanol-water mixture with a low percentage concentration of ethanol, that there is no clear trend on the basis of mass of zeolite or with time. This suggests that adsorption on the zeolite, if any, may not the only phenomenon being observed, but that some other process is also occurring. This for instance might be due to a loss of solution due to evaporation although the container was kept sealed during the experiment. Ethanol would evaporate preferentially. The quantities adsorbed are extremely small, if adsorption occurs at all and the experimental error is large compared to the changes being measured. It can be speculated why this occurs; but

the important conclusion with regard to this work is that no substantial adsorption takes place. Thus zeolite is not suitable for removing traces of ethanol from wastewater streams.

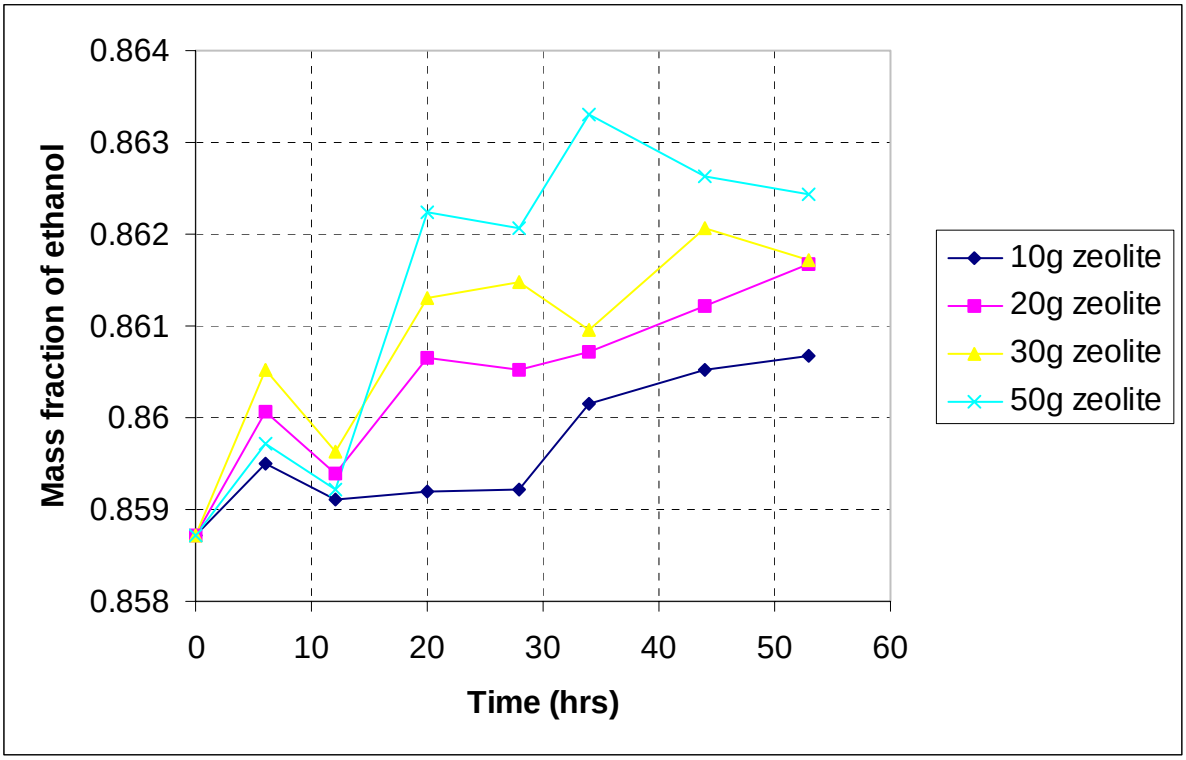

Figure 4.2 Changes in Ethanol Mass Fraction from an Initial Concentration of 85.9% Using Different Initial Masses of Zeolite

Figure 4.2 shows changes in mass fraction of ethanol from an initial value of 85.9 mass% ethanol for different masses of zeolite. An increase in mass fraction of ethanol in solution with time for various masses of zeolite is observed in Figure 4.2, which implies water is preferentially adsorbed on the zeolite. For 10, 20, 30, 50g mass of zeolite, the concentration of ethanol in solution increased by 0.21, 0.24, 0.24 and 0.36% respectively at 57hrs. As a result, it is worth investigating the mass of water adsorbed on the zeolite. A graph, which shows changes in water mass fraction, is plotted, as shown in Figure 4.3. The mass adsorbed is calculated on the basis of 85.9 mass% ethanol concentration and

the liquid phase concentration measured at a point in time. Detailed calculations are shown in Appendix D, Tables D2, D3, D4, D5 and D6.

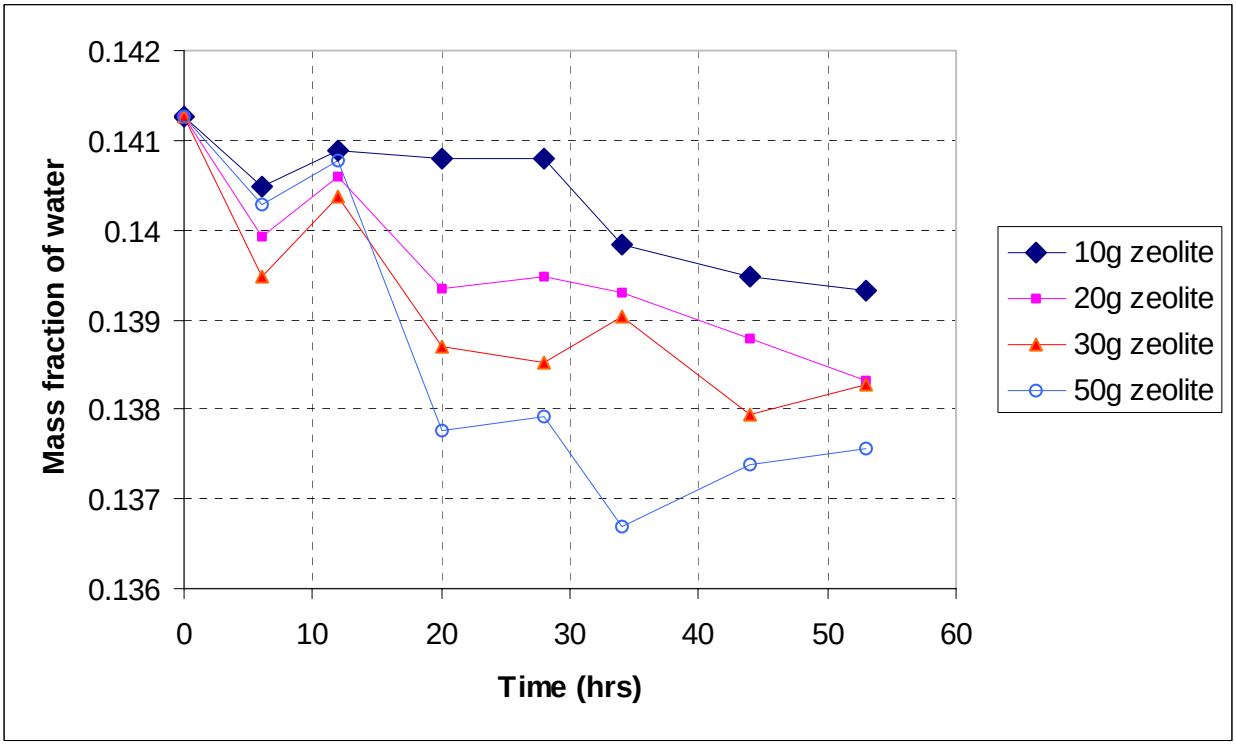

Figure 4.3 Changes in Water Mass Fraction in the Ethanol-Water Mixture with Time

It is evident from Figure 4.3 that the amount of water in the ethanol-water mixture decreases with time for the varying masses of zeolite. Moreover as the mass of zeolite increases the amount of water adsorbed also increases. Based on this observation, the graph of adsorption of water on Clinoptilolite from an initial 85.9 ethanol mass percent was plotted as shown in Figure 4.4.

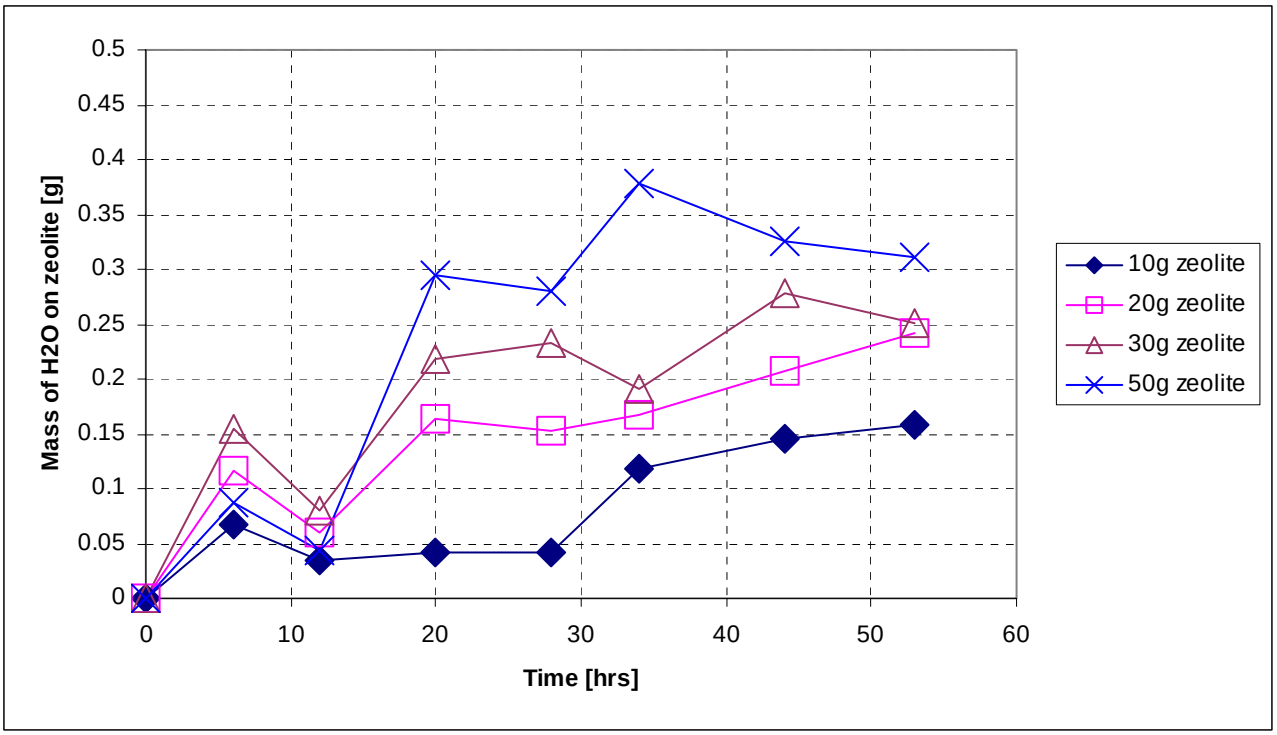

Figure 4.4: Adsorption of Water on Clinoptilolite from an Initial 85.8 % Ethanol Solution for Different Masses of Zeolite

From Figure 4.4, the relative mass of water adsorbed on the zeolite increases by 0.15, 0.25, 0.25 and 0.32g, as the mass of zeolite is increased to 10, 20, 30 and 50g, respectively. The trend of the graphs suggests that aqueous ethanol solution is being dehydrated, which suggests a potential use of South African Clinoptilolite.

However, the mass of water absorbed is by no means proportional to the mass of zeolite added. This might be due to the fact that the zeolite used in this work is in its natural state and contains various counter ions, which may affect adsorption. This means that further work would be required to upgrade the zeolite before it can be used for commercial applications.

4.3 Acetone Adsorption Screening Results

Yang, et al (1999) studied the adsorption of hydrocarbons, alcohols, ketones, organic acids, alkyl amines, chloro-organics and esters on a high silica faujasite (FAU) zeolite. The silica structure of faujasite exhibited a stronger affinity for acetone than ethanol. As already mentioned in Chapter 2 (refer to Section 2.2 and 2.3.2), Clinoptilolite is more highly siliceous than most natural zeolites, and hence it was worth investigating the adsorption of acetone on this zeolite.

The experimental results for both high and low concentrations of acetone are tabulated in Appendix D, Tables D7 and D8. The effect of the amount of zeolite added is investigated and the experimental results are plotted as shown in Figure 4.5 and 4.6. Figure 4.5 shows changes in acetone mass fraction from an initial 8.6 mass% acetone solution for different masses of zeolite and Figure 4.6 shows changes in acetone mass fraction from an initial 89.5 mass% acetone solution for different masses of zeolite.

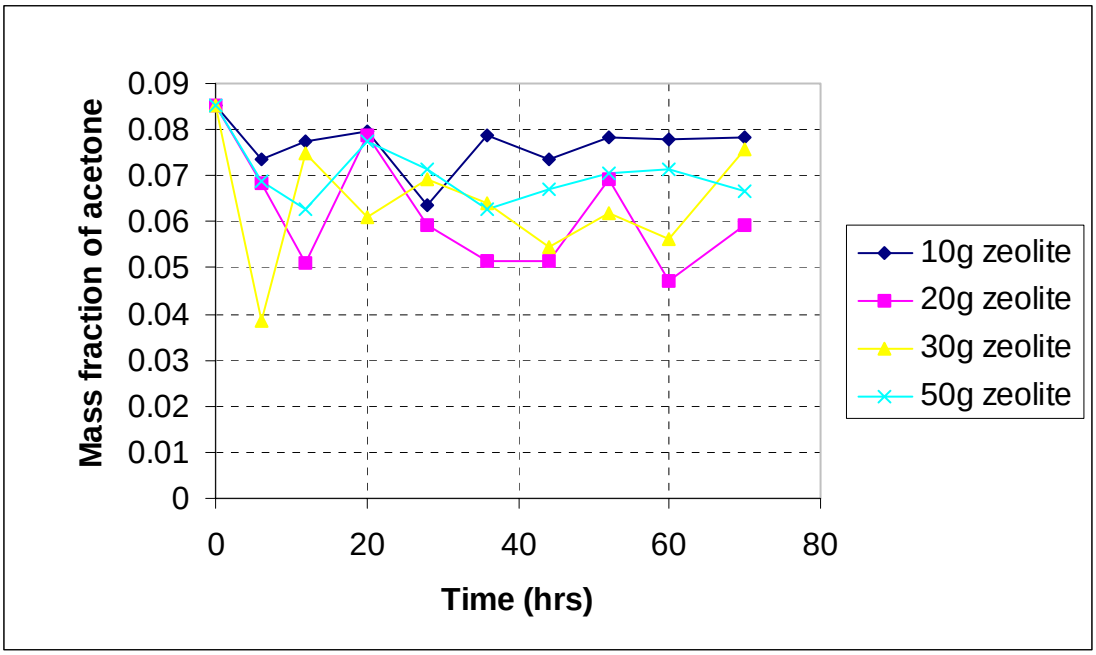

Figure 4.5 Changes in Acetone Mass Fraction with Time from an Initial 8.6% Acetone Solution Using Different Initial Masses of Zeolite.

For the low concentration acetone solution as shown in Figure 4.5, there is no clear trend on the basis of mass of zeolite. The adsorption of acetone relative to water is insignificant since the acetone mass fraction decreases from 8.6 to about almost 6 mass% for all masses of zeolite. As for the experiments using ethanol, a loss of solution due to evaporation may have occurred in spite of the fact that the container was kept sealed during the experiment. This could explain these results since acetone would evaporate preferentially. Nonetheless, it can be concluded that no substantial adsorption takes place. Since no notable adsorption was observed, it was decided that it was not worth pursuing this area of enquiry further.

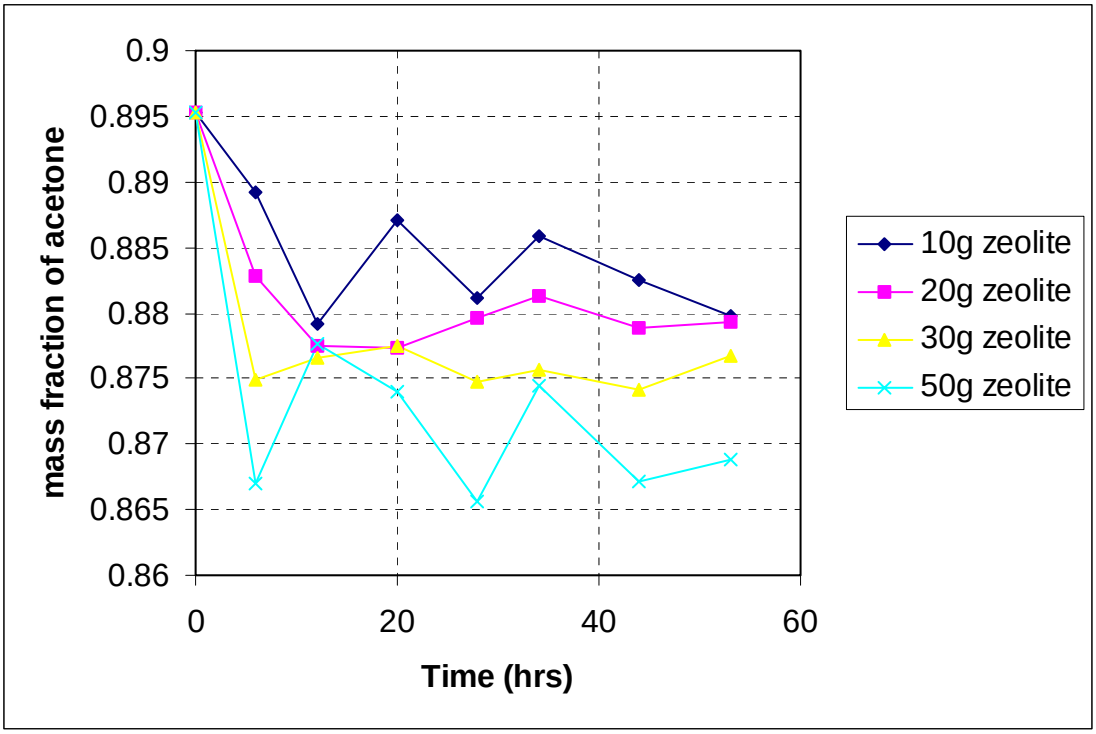

Figure 4.6 Changes in Acetone Mass Fraction from 89.5% Acetone Solution Using Different Initial Masses of Zeolite

For the high acetone concentration as shown in Figure 4.6, a trend on the basis of mass of zeolite used is observed. The mass fraction of acetone in the liquid phase drops with increasing mass of zeolite as observed from the graphs. These suggest that acetone is preferentially adsorbed over water onto the zeolite and hence it was worth investigating

this further. A plot of the mass of acetone on the zeolite is shown in Figure 4.7. The mass of acetone adsorbed on the zeolite was calculated by mass balance on the basis of the initial concentration and the liquid phase concentration measured at a point in time. Detailed calculations are shown in Appendix D, Tables D9, D10, D11 and D12.

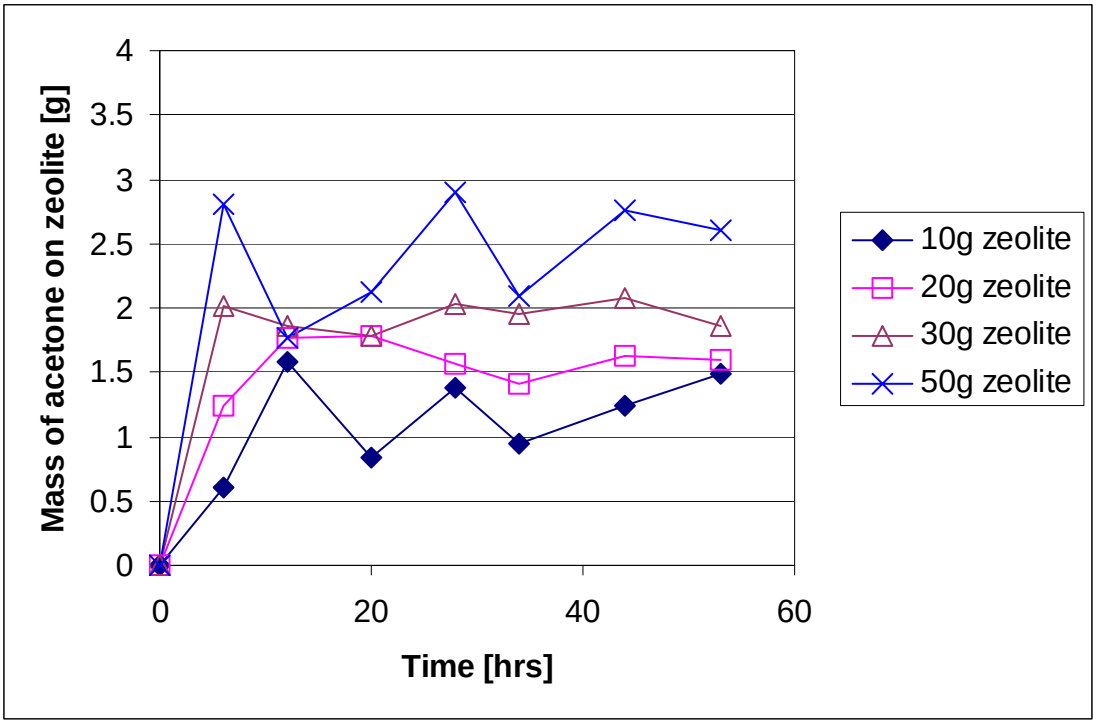

Figure 4.7 Adsorption of Acetone on Clinoptilolite from 89.5% Acetone Mass for Different Masses of Zeolite

The results suggest that there is insignificant adsorption of acetone onto the zeolite Clinoptilolite. The mass of water absorbed is by no means proportional to the mass of zeolite added. This suggests that in addition to adsorption on the zeolite, some other process is also occurring, for example the loss of acetone due to preferential evaporation. It might also be due to differential adsorption by the material. The matter was however, not pursued further as the results were not sufficiently interesting to warrant further work. Furthermore, too small an amount of acetone was adsorbed onto the zeolite relative to the 85.8 initial mass %, to suggest any practical potential commercial application.

4.4 Concluding Remarks

The results reveal that South African Clinoptilolite is not a good adsorbent for removing acetone and ethanol from aqueous solutions with low concentrations of acetone and ethanol. Thus it would not be suitable for use in wastewater treatment of aqueous streams with traces of acetone and ethanol. However, it can be concluded from the results that Clinoptilolite has a potential of removing water from organic molecules such as ethanol, but not acetone. This is probably due to the hydrogen bonding which occurs between acetone and water, but not between acetone molecules on their own, unlike ethanol. The results obtained in this work are in agreement with those reported in the literature (Tihmillioglu and Ulku, 1996) for the adsorption of water.

The dehydration of aqueous organic solutions by South African Clinoptilolite seems to have a promising future and might be of possible use in purification of high-grade chemicals, or in petrol stations as a drying agent. However, the adsorption effect of the adsorbate is small and hence further work, such as preconditioning the zeolite and upgrading the zeolite before it can be used commercially, is required.

4.5 Metal Ions Adsorption

This section reports and discusses the experimental results obtained from screening for possible removal of metal ions from water. The metal ions investigated in this work are Zn^{2+}, Ni^{2+} and $Pb^{2+,}$ as already mentioned in Section 3.3.8.1. The initial concentration used for the investigation of Zn^{2+}, Ni^{2+} and Pb^{2+} is 45 mg/L and the volume of the aqueous solution is 100 mL. The experimental results obtained are compared with related work as reported in the literature.

4.5.1 Adsorption of Zn^{2+} on Clinoptilolite

The experimental results showing the changes in zinc concentration from an initial concentration of 45 mg/L with time for varying masses of zeolite using Clinoptilolite are tabulated in Appendix E (Table E1) and are plotted as shown in Figure 4.8.

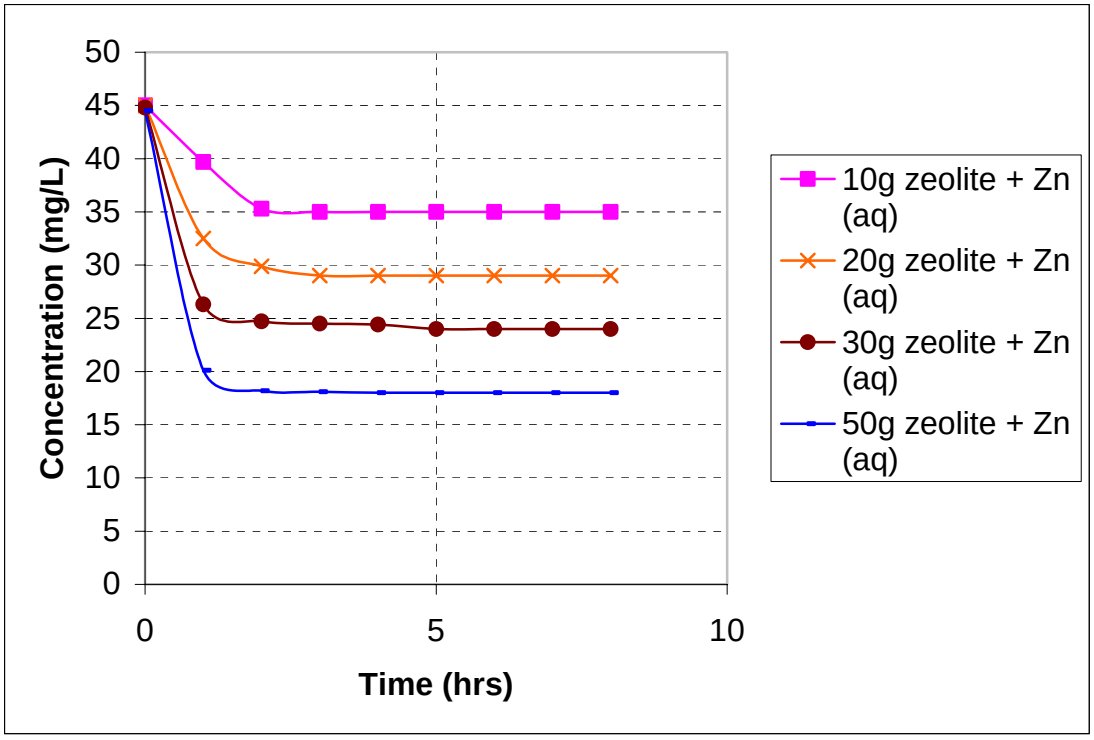

Figure 4.8 Change in Zinc Concentration with Time from 45 mg/L Using

Various Masses of Zeolite

It can be observed from Figure 4.8 that the initial zinc concentration reduces quickly initially then levels off with time for all experiments. As the amount of zeolite is increased, the final concentration of Zn^{2+} decreases, which implies that the zinc metal ion is ion exchanged onto the zeolite. This implication has necessitated the calculation of the loading of zinc on the zeolite to observe the amount of the metal ion on the zeolite.

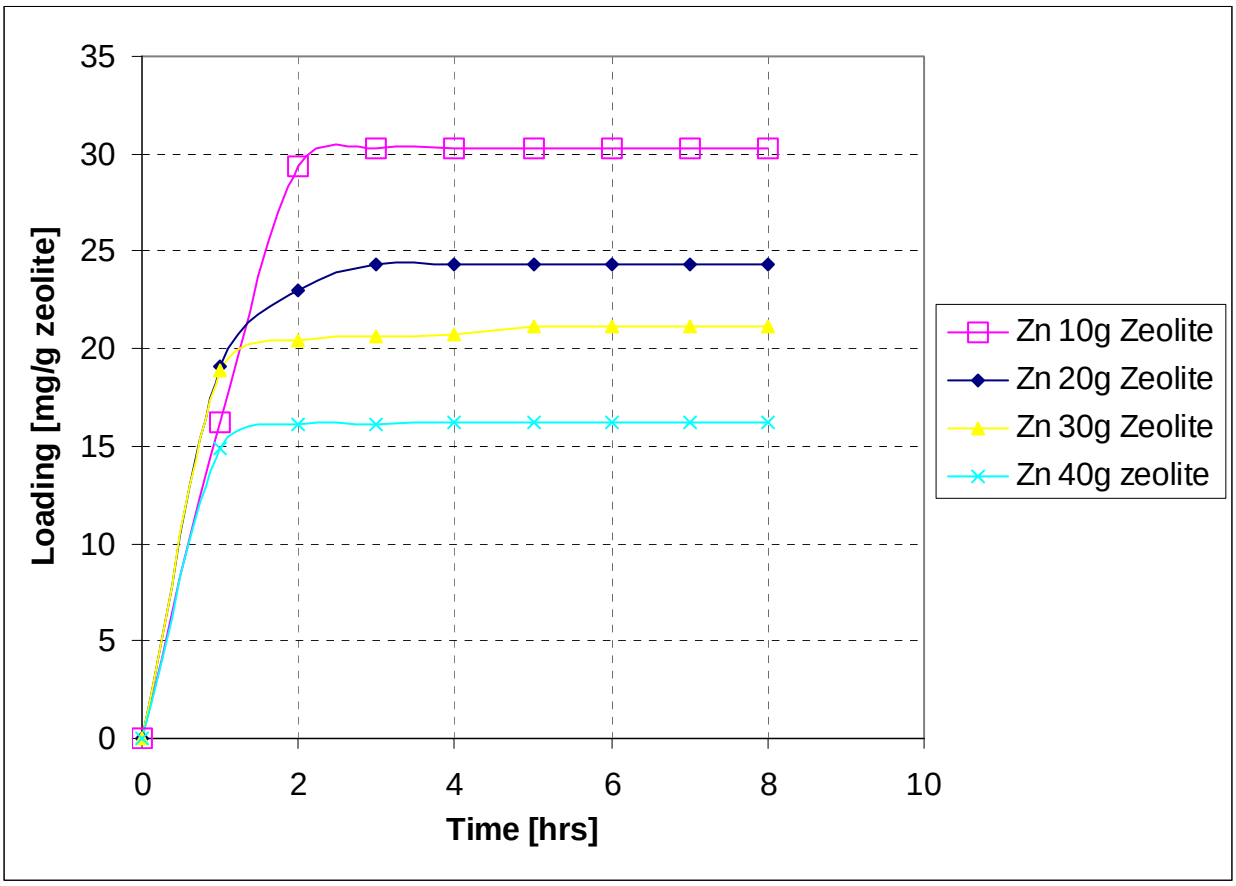

Figure 4.9 Loading of Zn^{2+} on Clinoptilolite

The amount of Zn^{2+} on the zeolite is calculated by mass balance and the results are tabulated in Appendix E (Table E4). Figure 4.9 shows the amount of Zn^{2+} on zeolite (mg/g) against time for various masses of zeolite. The uptake of Zn^{2+} ranges from 30.28 to 16.18 mg/g for 10 to 50g mass of zeolite, respectively, and these results are tabulated in Table 4.1.

Table 4.1 Zn^{2+} Uptake

Mass of zeolite (g)	**mg/g**
10	30.28
20	24.34
30	21.13
50	16.18

This suggests that there is an equilibrium between the adsorbed material and that remaining in solution. Equilibrium is reached in about 3 hours, irrespective of the mass of zeolite used. This means that film diffusion is not the rate-limiting step. It is also noted that for a fixed volume of a solution for varying mass of zeolite, the loading onto the zeolite decreases with increasing mass of zeolite. These results warranted an investigation on Zn^{2+} adsorption isotherms.

4.5.1.1 Zn^{2+} Adsorption Isotherms

The plotting of adsorption isotherms is a conventional method of presenting adsorption equilibria. An adsorption isotherm describes the distribution of the adsorbate (Zn^{2+} in this section) between the aqueous solution and the adsorbent (here the natural zeolite). The experimental data were linearised in the form of Langmuir adsorption isotherm as discussed in section 2.3.3 by plotting C_e/Q_e against C_e. The Langmuir constants X_m and K were evaluated from the slope and intercept of the linear equation.

Where Q_e = the quantity of adsorbate per unit weight of adsorbent
(mg Zn^{2+} per g of Clinoptilolite in this case),
and C_e = the concentration of adsorbent remaining in solution
(mg/L, Zn^{2+}).

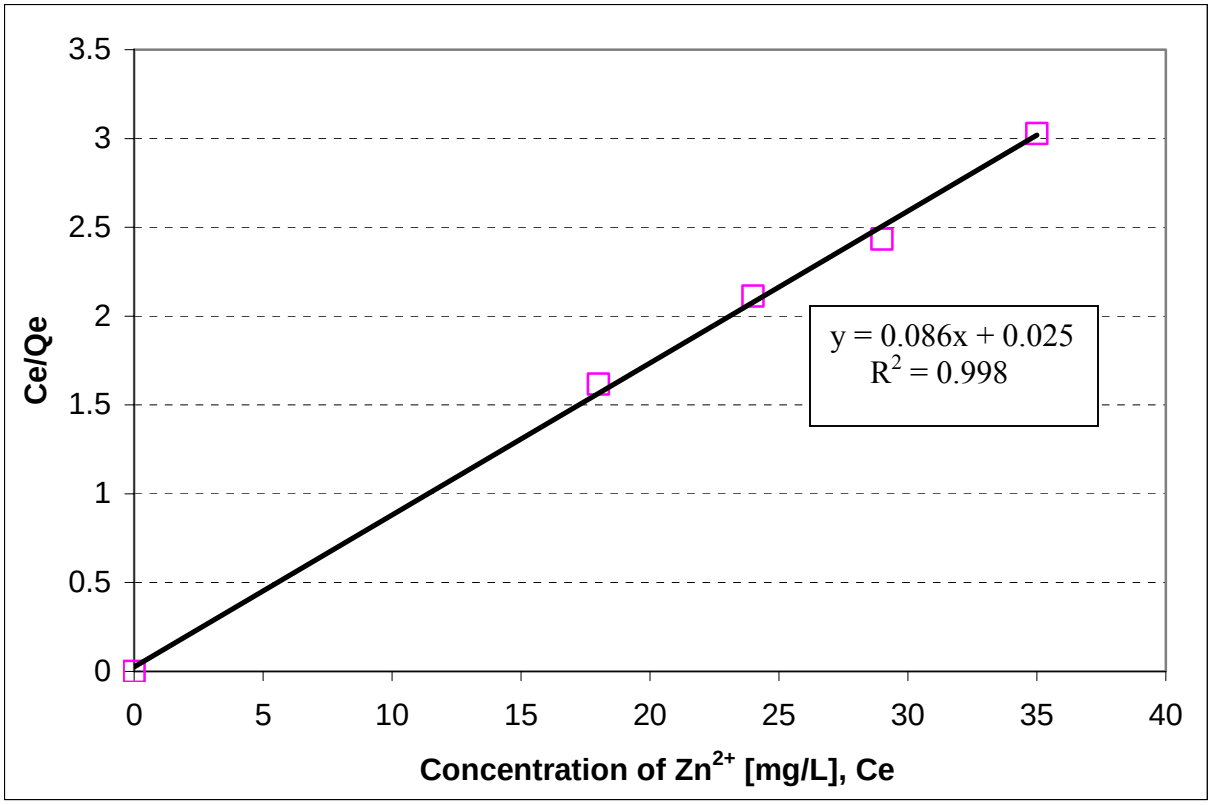

Figure 4.10 Isotherm for the Adsorption of Zn^{2+} on Clinoptilolite

Figure 4.10 represents an isotherm for the adsorption of Zn^{2+} on Clinoptilolite, which is obtained by plotting C_e/Q_e against C_e. A linear isotherm is observed which means the concentration of Zn^{2+} in solution is proportional to the loading of Zn^{2+} per gram of zeolite. The linear equations and correlation coefficients for the isotherms are summerised and tabulated in appendix H (Table H3 and H4). These results (and the fact that the regression coefficient for the plot of C_e/Q_e against C_e is 0.998, indicating good linearity) confirm that the adsorption of Zn^{2+} on zeolite follows the Langmuir adsorption isotherm. The Langmuir constant X_m (maximum adsorption capacity) and K (Langmuir constant related to energy of adsorption) are evaluated from the slope and the intercept of the linear equation and were found to be 11.69 and 0.29 respectively.

4.5.2 Adsorption of Ni^{2+} on Clinoptilolite

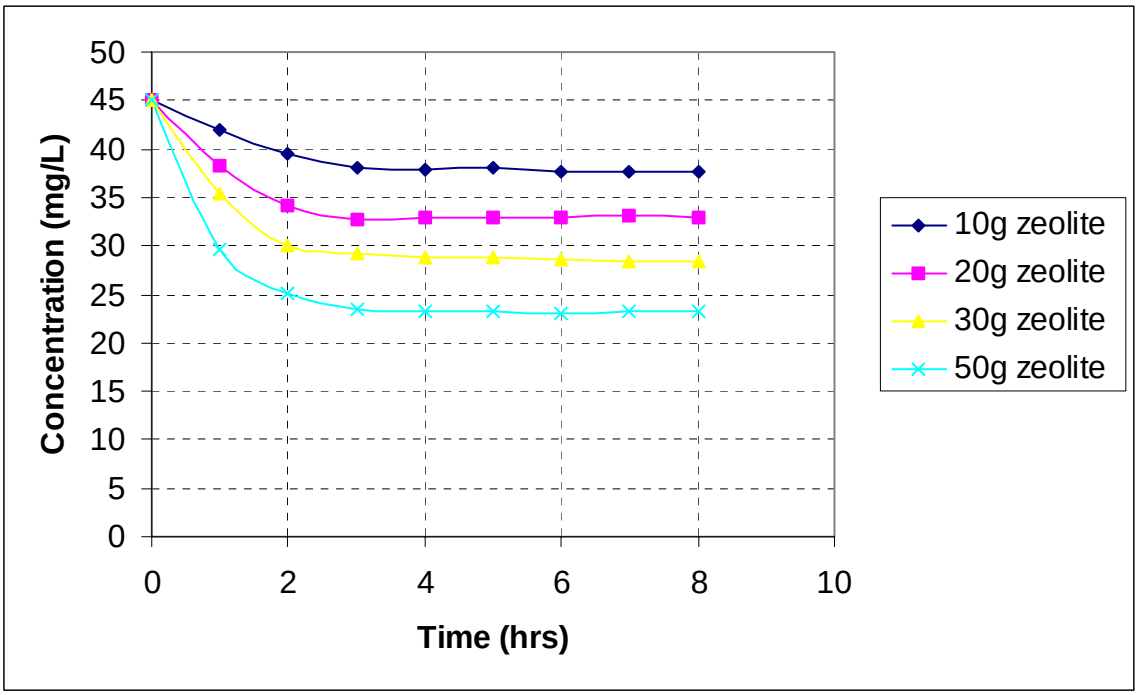

Figure 4.11 Changes in Ni^{2+} Concentration with Time from an Initial Concentration of 45 mg/L Using Various Masses of Zeolite

Figure 4.11 shows the adsorption of Ni^{2+} on Clinoptilolite and the effect of the amount of zeolite on the adsorption of Ni^{2+}. In the figure, changes in Ni^{2+} concentration from an initial concentration of 45 mg/L for various masses of zeolite are plotted against time. The experimental data used to plot the above figure is tabulated in the Appendix F (Table F1).

It is apparent from the figure that Ni^{2+} ions are adsorbed for all the masses of zeolite. The results also indicate that as the amount of zeolite is increased, the final concentration of Ni^{2+} decreases. This is agreement with the study conducted by Zorpas and Loizidou, (1999). Although their study was conducted with Clinoptilolite from Greece that was dried in an oven, they found that Clinoptilolite has the ability to take up nickel ions and

they also found that when the amount of zeolite is increased, the final concentration decreases.

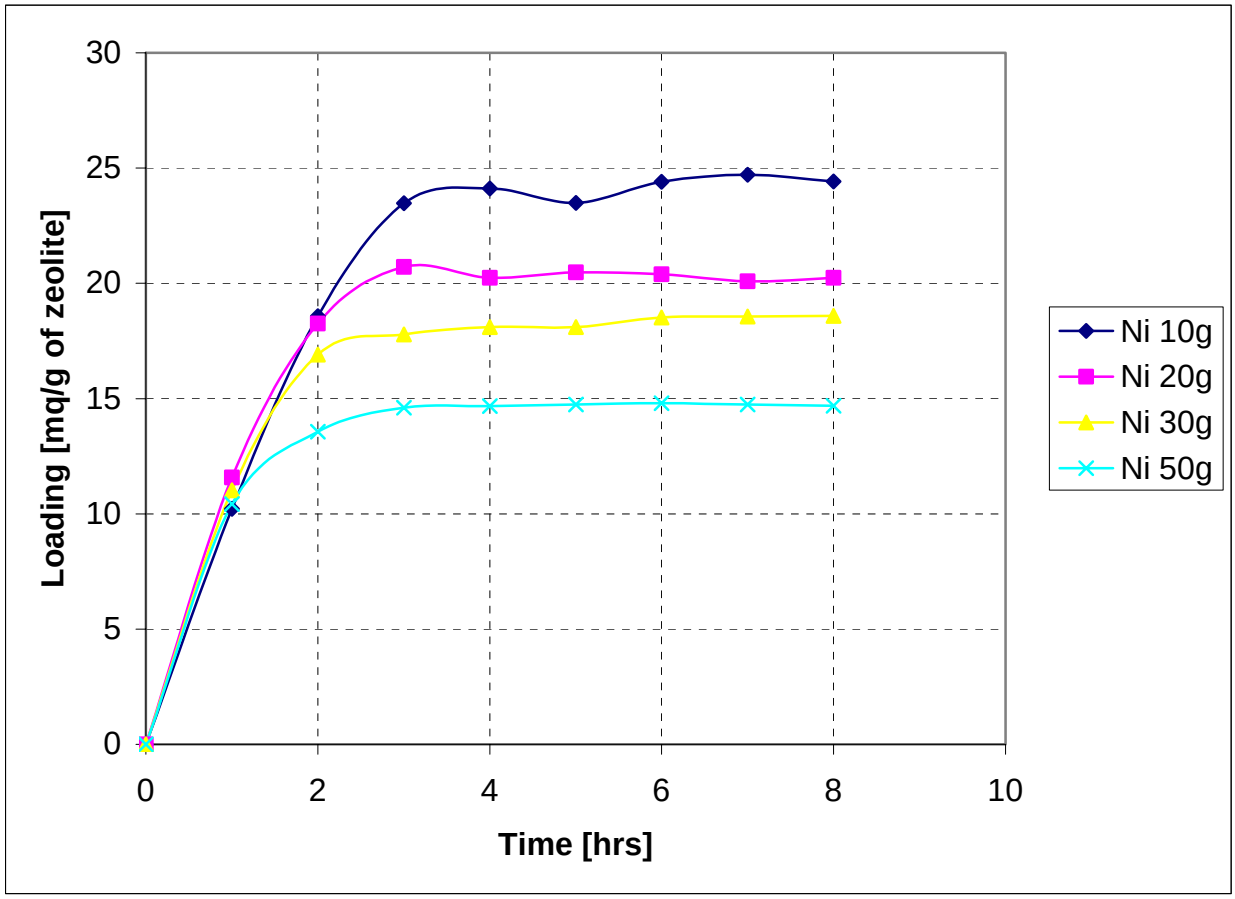

Figure 4.12 Loading of Ni^{2+} on Clinoptilolite

The amount of Ni^{2+} on the zeolite is calculated by mass balance and the results are tabulated in Appendix F (Table F4). Figure 4.12 shows the amount of Ni^{2+} on zeolite against time for various masses of zeolite. The uptake of Ni^{2+} ranges from 24.42 to 14.68 mg/g for 10 to 50g of zeolite, respectively, as shown in Table 4.2.

Table 4.2 Ni^{2+} Uptake

Mass of Zeolite	**mg/g**
10	24.42
20	20.24
30	18.59
50	14.68

This suggests that there is an equilibrium between the adsorbed material and that remaining in solution. The loading amount of Ni^{2+} onto the zeolite decreases as the mass of zeolite increases for the same volume of solution. Equilibrium is reached in approximately 5 hours, irrespective of the mass of zeolite. The results warranted an investigation of Ni^{2+} adsorption isotherms.

4.5.2.1 Ni^{2+} Adsorption Isotherm

Figure 4.13 shows an isotherm for the adsorption of Ni^{2+} on Clinoptilolite, which is obtained by plotting C_e/Q_e against equilibrium concentration C_e. A linear isotherm is observed which means the concentration of Ni^{2+} in solution is proportional to the loading of Ni^{2+} per gram of zeolite. The linear equations and correlation coefficients for the isotherms are summerised and tabulated in Appendix H (Table H3 and H4). These results (and the fact that the regression coefficient for the plot of C_e/Q_e against C_e is 0.997, indicating good linearity) confirm that the adsorption of Ni^{2+} on zeolite can be modeled by the Langmuir adsorption isotherm. The Langmuir constant X_m (maximum adsorption capacity) and K (Langmuir constant related to energy of adsorption) are evaluated from the slope and the intercept of the linear equation and were found to be 15.8 and –0.052, respectively.

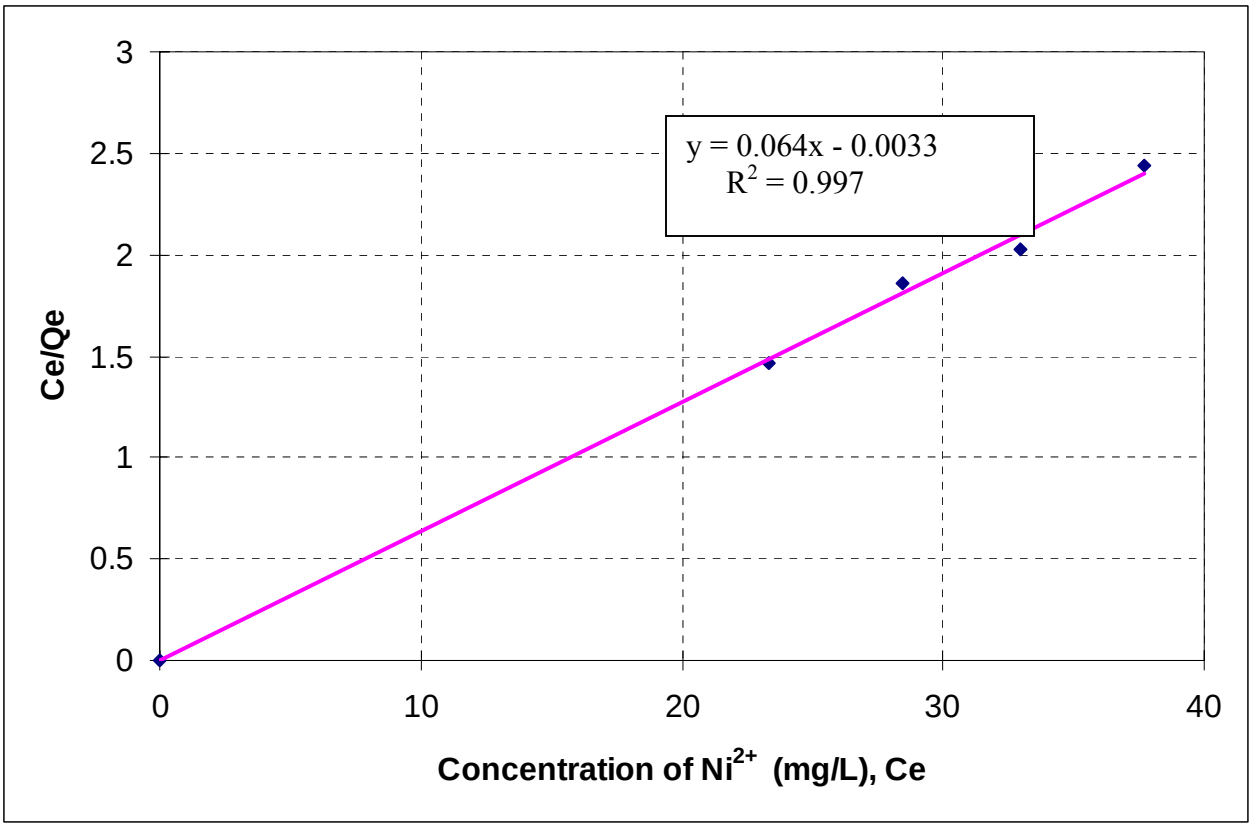

Figure 4.13 Isotherm for the Adsorption of Ni^{2+} on Clinoptilolite

4.5.3 Adsorption of Pb^{2+} on Clinoptilolite

The experimental results showing changes in lead concentration from an initial concentration of 45 mg/L for varying masses of zeolite with time. The results are tabulated in appendix G (Table G1) and are plotted in Figure 4.14. It can be observed from the figure that after 3 hours the lead concentration falls to below 10 mg/L for all the masses of zeolite used. This implies that South African Clinoptilolite has strong affinity for lead. It can also be noted that the aqueous solutions equilibrate after approximately 3 hours in all experiments.

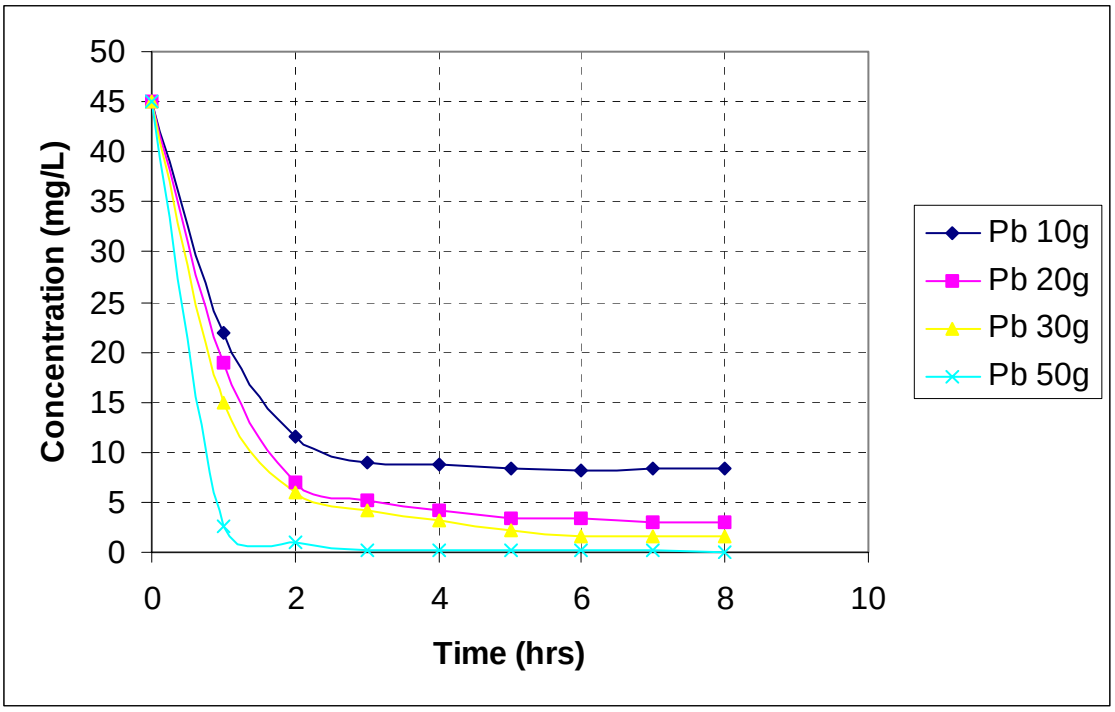

Figure 4.14 Changes in Lead Concentration with Time from an Initial Concentration of 45 mg/L Using Various Masses of Zeolite

The amount of Pb^{2+} on the zeolite is calculated by mass balance and the results are tabulated in Appendix G (Table G4). Figure 4.15 shows the amount of Pb^{2+} on zeolite against time for various masses of zeolite. The uptake of Pb^{2+} ranges from 35.05 to 8.67 mg/g for 10 to 50g mass of zeolite as shown in Table 4.3.

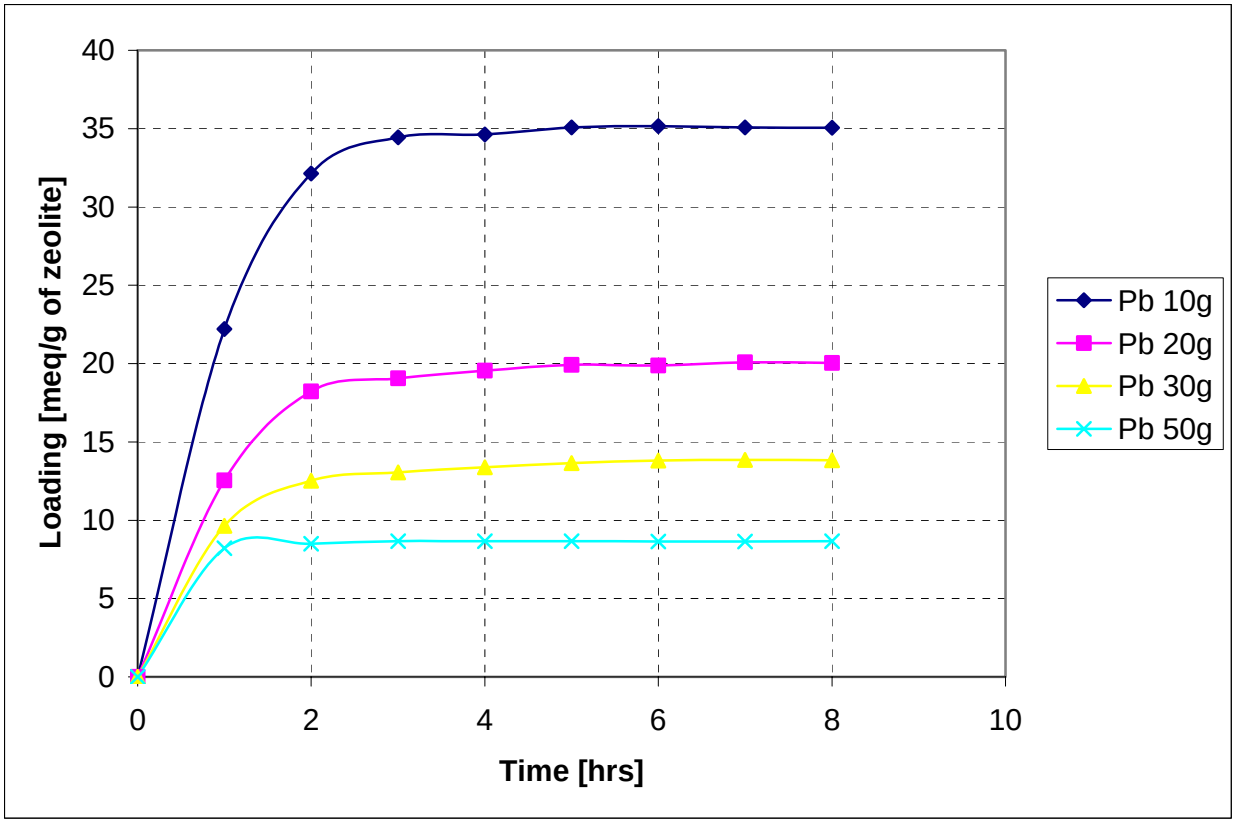

Figure 4.15 Loading of Pb^{2+} on Clinoptilolite

Table 4.3 Pb^{2+} Uptake

Mass of Zeolite	**mg/g**
10	35.05
20	20.04
30	13.83
50	8.67

This suggests that there is an equilibrium between the adsorbed material and that remaining in solution. The amount of Pb^{2+} in solution decreases as the mass of zeolite increases for the same volume of solution. As noted for Zn^{2+} equilibrium is attained after about 3 hours and this is independent of the mass of zeolite used. The results warranted an investigation of Pb^{2+} adsorption isotherms.

4.5.3.1 Pb^{2+} Adsorption Isotherm

The adsorption isotherm for Pb^{2+} as a function of solute concentration is shown in Figure 4.16. The experimental data were analysed by plotting C_e/Q_e against C_e and is tabulated in Appendix H.

Where Q_e = the quantity of adsorbate per unit weight of adsorbent
($mg\ Pb^{2+}$ per g of Clinoptilolite in this case),
and C_e = the concentration of adsorbent remaining in solution at equilibrium
($mg/L\ Pb^{2+}$).

Figure 4.16 shows an isotherm for the adsorption of Pb^{2+} on Clinoptilolite, which is obtained by plotting C_e/Q_e against the final equilibrium concentration C_e.

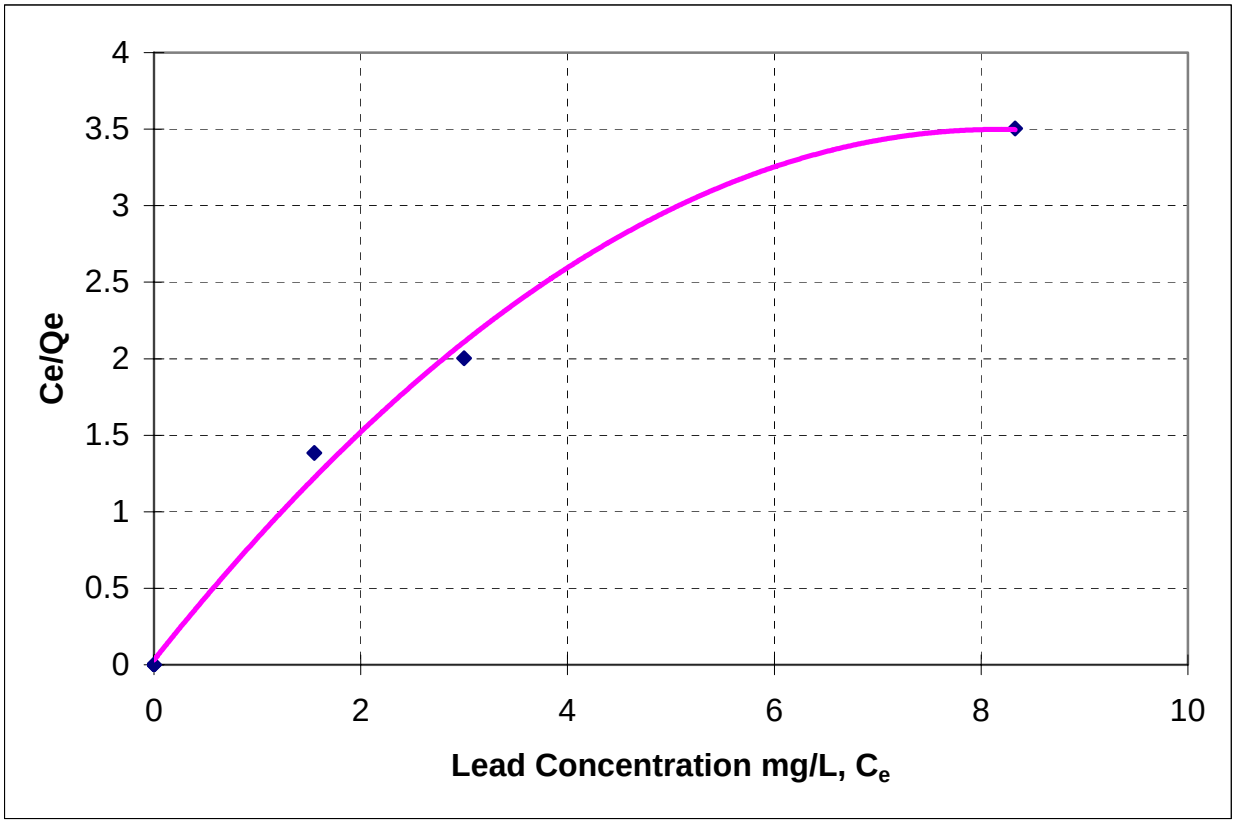

Figure 4.16 Pb^{2+} Adsorption Isotherm

A non-linear isotherm is observed which means the concentration of Pb^{2+} in solution is not proportional to the loading of Pb^{2+} per gram of zeolite, and the adsorption of Pb^{2+} on zeolite does not follow the Langmuir theory of adsorption. Therefore, another commonly used adsorption isotherm, the Freundlich adsorption isotherm, was assessed to investigate whether the adsorption of Lead on Clinoptilolite could be fitted using this model instead.

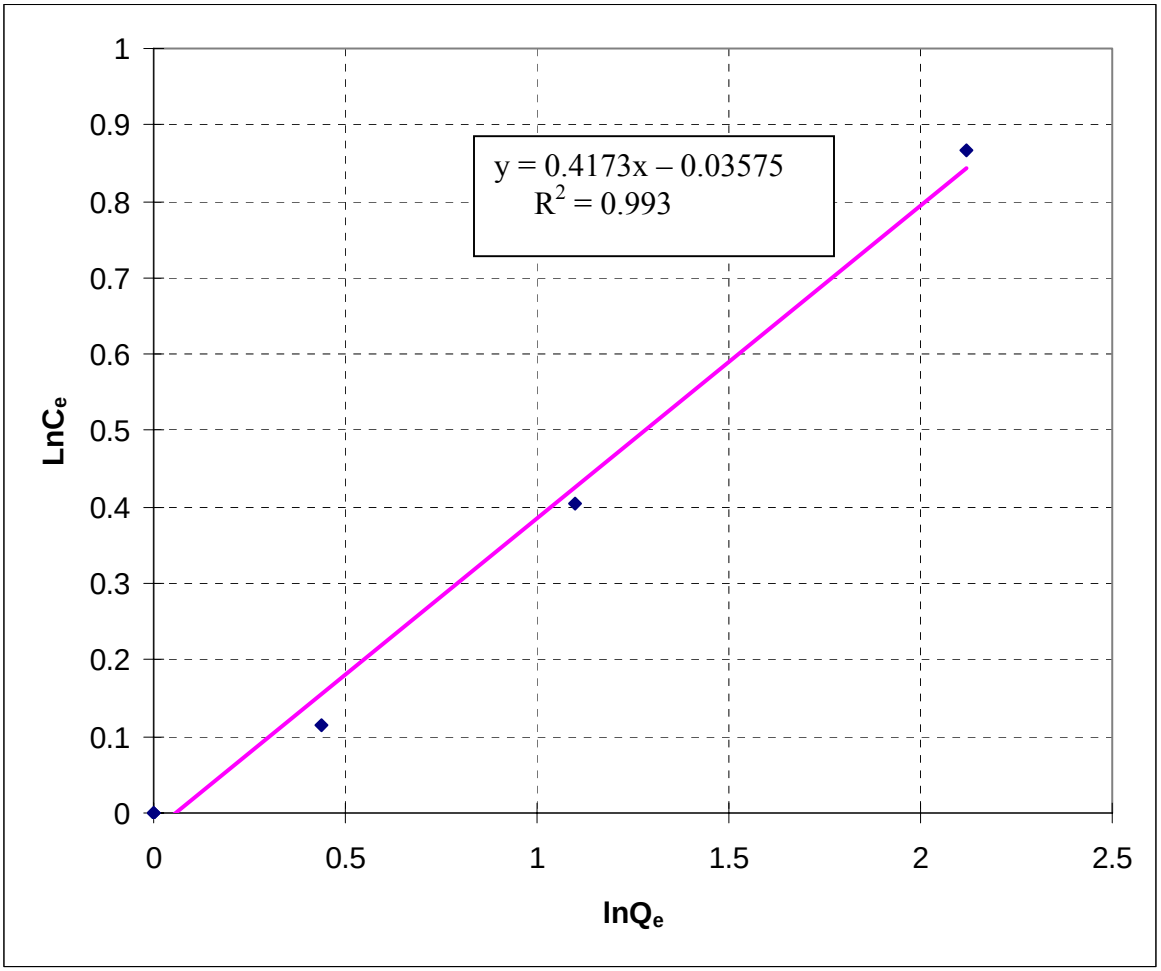

Figure 4.17 Freundlich Adsorption Isotherm Pb^{2+}

Figure 4.17 shows the Freundlich adsorption isotherm for the adsorption of Pb^{2+} on Clinoptilolite. The isotherm was obtained by plotting $\ln C_e$ against $\ln Q_e$. The plot yielded

a straight line. The Freundlich constant K_f (an empirical constant) is evaluated from the intercept of the linear equation and is found to be 0.956 and is tabulated in appendix H (Table H3 and H4).

It appears that Pb^{2+} is held more strongly by the zeolite than the other cations investigated. Since the concentration has been measured in ppm (or mg/L), the molar concentration of Pb^{2+} is very low. In the light of the low concentration the Clinoptilolite shows exceptionally high affinity for Pb^{2+}. This indicates that Pb^{2+} is irreversibly adsorbed and therefore poses a serious challenge for the regenerability of the zeolite once it has been used to remove Pb^{2+} in commercial application.

4.5.4 Metal Ions Selectivity

The adsorption Isotherms of Zn^{2+}, Ni^{2+} and Pb^{2+} were plotted on the same graph as shown in Figure 4.18. As already mentioned the Pb^{2+} adsorption isotherm does not yield a straight line, implying that it does not obey Langmuir adsorption theory. However, the isotherms for Zn^{2+} and Ni^{2+} do yield straight lines and obey Langmuir adsorption theory.

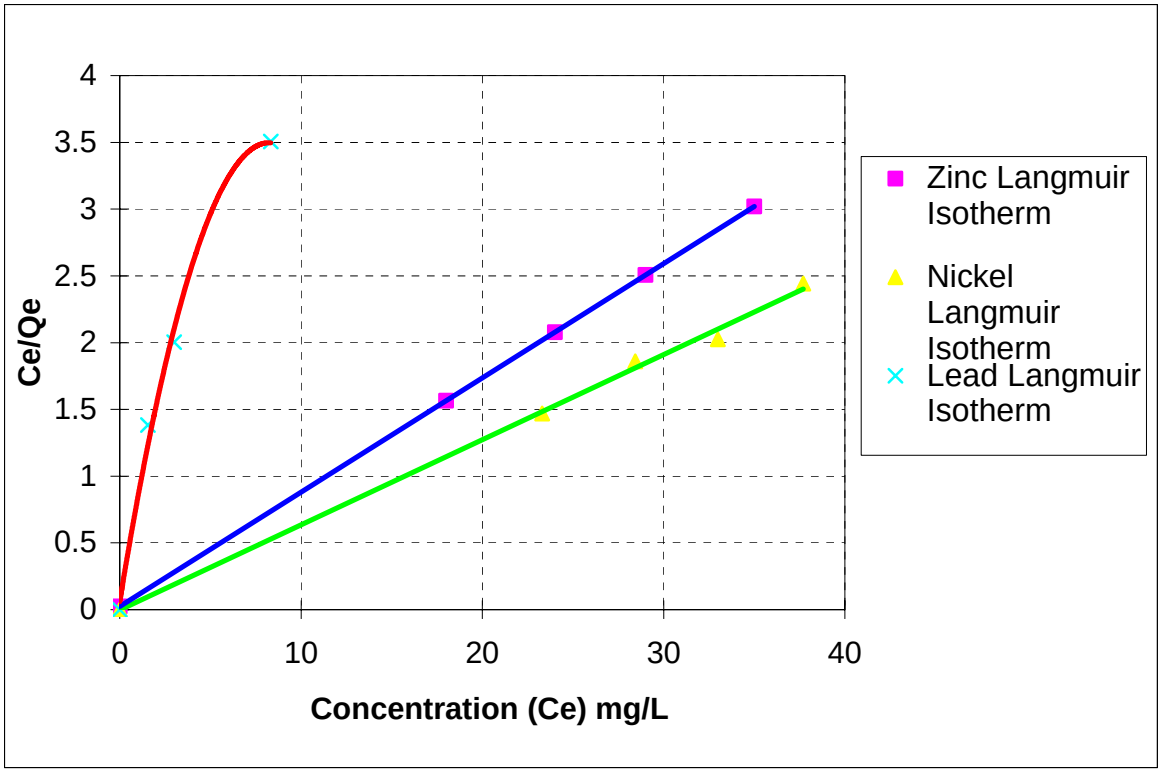

Figure 4.18 Metal Adsorption Isotherms

The slope of the adsorption isotherm of metal ions increases in the order of Ni^{2+}, Zn^{2+} and Pb^{2+}. The Pb^{2+} isotherm plot has considerably higher slope than the other two metals. Furthermore, the concentration of the Pb^{2+} left in a solution at equilibrium is 8.67 mg/L, which is significantly lower compared with that of Ni^{2+} and Zn^{2+}, which range between 15 and 30 mg/L

This means that the selectivity of the zeolite for the adsorption in decreasing order is Pb^{2+}, Zn^{2+} and Ni^{2+}. It is interesting to note that the ionic radii of Pb^{2+}, Zn^{2+} and Ni^{2+} are 1.19 Å, 0.74 Å and 0.69 Å, respectively (Lee, 1991). It appears that as the ionic radius of the metal ion increases the more that ion is preferred by the zeolite. This is contrary to expectations; one expects smaller ions to diffuse into the zeolite with greater ease resulting in a higher selectivity. Thus, the selectivity is probably due to the difference in the hydrated radii; in general the smaller the ion, the higher the charge density and the greater its hydrated radius.

The selectivity series for cations could be attributed to the necessity to reject some of the water molecules of the highly hydrated ions to permit diffusion of the ions through the specific zeolite structure (Inglezakiz et al, 2004). In Table 4.4 hydration energies in water of the three heavy metal ions in aqueous solutions at 25^0C are shown (Marcus, 1991). The concept of rejection of some water molecules, which is related to the hydration energies of the cations, does explain the high selectivity for Pb^{2+} and the lower selectivity for Zn^{2+} and Ni^{2+}. This is possibly the reason that the selectivity increases in the way that it does. Similar observations have been made by other authors, where selectivity of natural zeolite could be dictated by energy of hydration of cations (Dal Bosco et al, 2005; Inglezakiz et al, 2004).

Table 4.4 Hydration energy of metals in water

Metal ion	**Gibbs energies of hydration of ions (kJ/mol)**
Ni^{2+}	-1980
Zn^{2+}	-1955
Pb^{2+}	-1425

It is encouraging that Clinoptilolite is able to ion exchange heavy metal ions from solution with a reasonably favourable equilibrium. However, it may not be possible to regenerate Clinoptilolite, as certain ions seem to be very strongly adsorbed. This would probably make it unsuitable as an ion-exchanger for commercial applications. As a result of this work, further work was carried out by Moshesh and Ntlango (2004) as a final year project. Their report is given in Appendix I. They investigated the regenerability of Clinoptilolite loaded with Cu^{2+} and Fe^{2+}.

The zeolite, loaded with Cu^{2+} and Fe^{2+} metal ions was washed with distilled water to remove the ions that are not adsorbed onto the zeolite. The regeneration of the zeolite was achieved by exposing it to a sodium chloride solution over a period of 3 to 7 days. Cu^{2+} and Fe^{2+} metal ions were then recovered from the zeolite.

4.5.5 Adsorption Capacity of Virgin and Regenerated Clinoptilolite

Figure 4.19 and 4.20 shows the loading capacity of virgin and regenerated Clinoptilolite for different masses of zeolite. The loading capacity of both regenerated and virgin Clinoptilolite for the adsorption of both copper and iron ions decreases for higher masses of zeolite. The adsorption capacity of the regenerated zeolite is lower than the virgin zeolite for all masses of the zeolite. The difference in loading capacity of virgin and regenerated Clinoptilolite is the same for all varying masses of zeolite.

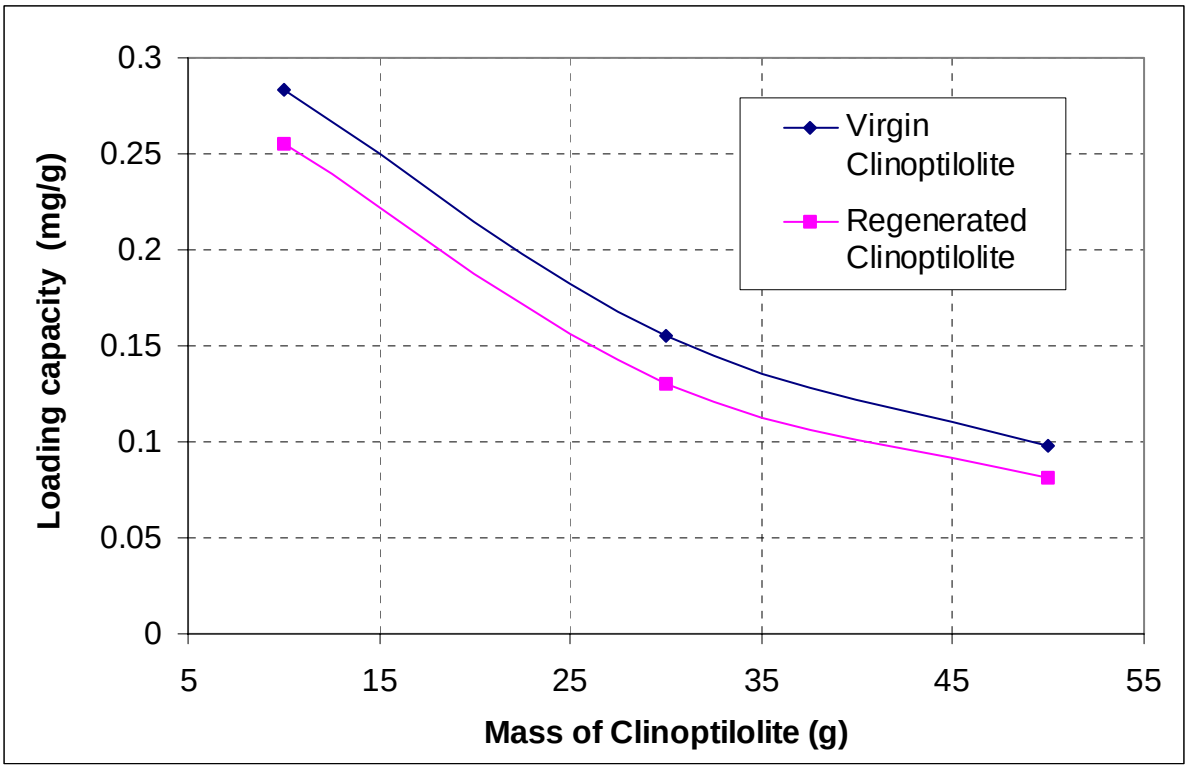

Figure 4.19 Loading Capacity of Clinoptilolite for Cu^{2+} (Moshesh and Ntlango, 2004)

The adsorption capacity of Clinoptilolite appears to decrease as the mass of zeolite increases. The decrease in loading capacity is more rapid at small masses of Clinoptilolite than at high masses.

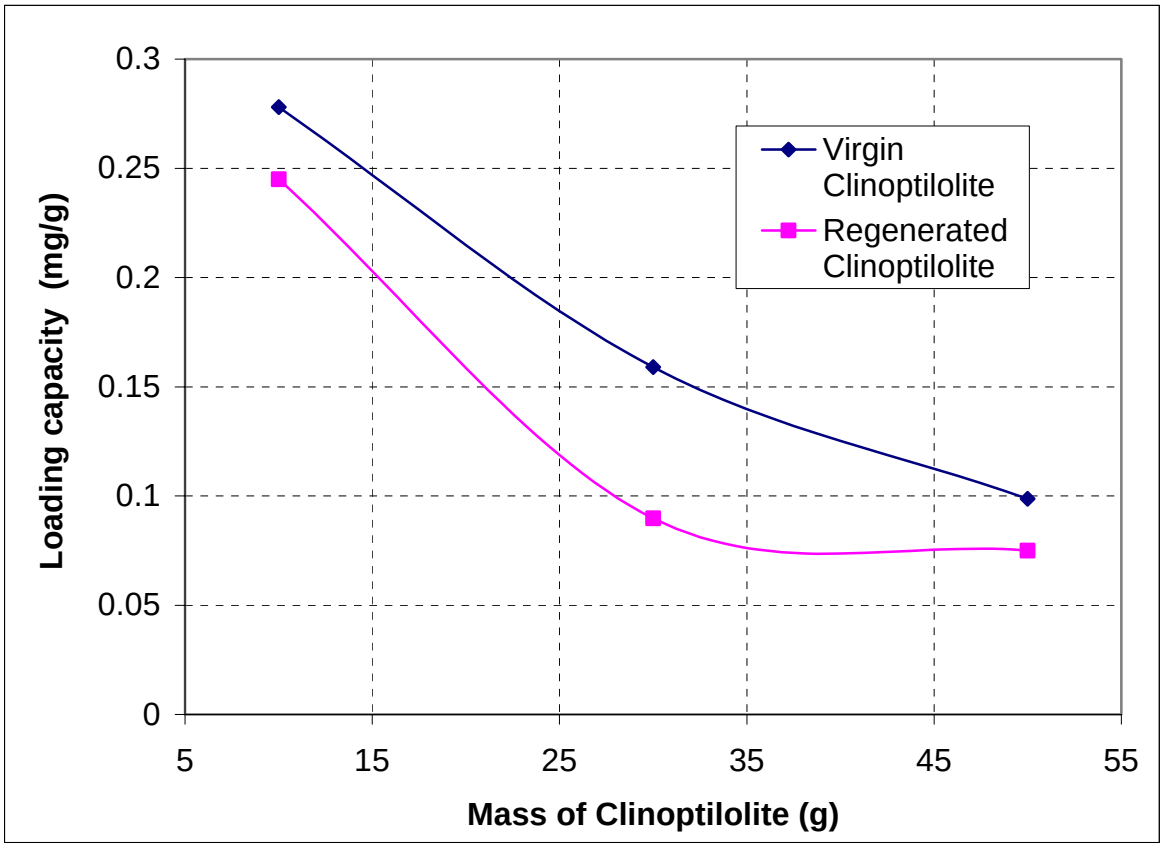

Figure 4.20 Loading Capacity of Clinoptilolite for Fe^{2+} (Moshesh and Ntlango, 2004)

For both Cu^{2+} and Fe^{2+} at all masses of zeolite considered, the same initial volume of solution and concentration of metal was used, i.e. 50ppm (see Appendix I). The small mass of zeolite removes only a small amount of the metal in solution, leaving a higher concentration of metal ions in solution. From the isotherms it is known that the higher solution concentration results in higher loading at equilibrium. This is the reason that more metal is loaded onto the zeolite when smaller masses are used.

The graphs for virgin and regenerated zeolite are slightly further apart for the experiment in which Fe^{2+} was loaded, than that in which Cu^{2+} was loaded. This suggests that the regenerated capacity will vary depending on the metal ion loaded on the zeolite. This is probably an indication that the selectivity of the zeolite for Fe^{2+} is greater than for Cu^{2+} enabling the Fe^{2+} to displace more of the ions originally present in the zeolite with each successive adsorption step.

4.5.6 Concluding Remarks

The zeolite exhibited exceptional selectivity for the removal of lead compared to other metals. The selectivity for the uptake of the metals in decreasing order was lead, zinc and lastly nickel.

The study carried out by Moshesh and Ntlango (2004) has shown that Clinoptilolite can be regenerated using high concentrations of sodium chloride and can be re-used to absorb metal ions. The adsorption capacity of Clinoptilolite decreases with each successive regeneration and re-use of the zeolite. Moreover, how the capacity drops may be dependent on the metal ion adsorbed on the zeolite. Further work needs to be done to investigate the regenerability of zeolite loaded with lead, zinc and nickel, in addition to improving the regeneration process to increase the lifespan of the zeolite. Therefore, provided that the zeolite loaded with these metal ions can be regenerated and can be reused, it could be used for effluent treatment in mining activities that have traces of lead, and in the battery industry.

Chapter 5 Conclusion and recommendations

The ability of South African natural zeolite, Clinoptilolite, to remove oxygenated organic molecules and heavy metal ions from water was investigated by carrying out simple, quick batch experiments under ambient conditions.

Oxygenated organic molecules such as ethanol and acetone were considered in this work as they do not form two-phase mixtures with water. Solutions with high and low concentrations of ethanol and acetone were studied. The zeolite was found to be unsuitable for the adsorption of acetone and ethanol due to preferential adsorption of water. As a result, the potential of the zeolite as a drying agent for ethanol and acetone was tested. It was found that the zeolite could find application in the dehydration of ethanol, but not of acetone.

The heavy metal ions considered in this work are lead, zinc and nickel. The effect of the mass of Clinoptilolite on the uptake of heavy metal ions was investigated and an adsorption isotherm was plotted for each metal. In addition, the isotherm of each metal was plotted on the same graph to determine the selectivity of Clinoptilolite for the metal ions.

The zeolite exhibited exceptional selectivity for the removal of lead, and reduced the concentration of lead in the water to levels below detection by Atomic Adsorption. The selectivity for the uptake of the metals in decreasing order was lead, zinc and lastly nickel. Therefore, provided the zeolite can be regenerated, it could be used for effluent treatment in mining activities that have traces of lead in the ore body such as occurs in zinc and silver deposits and in the battery industry.

As a result of the work presented in this dissertation, a further project was undertaken to investigate the regeneration of the zeolite and this project is reported in Appendix I. Preliminary findings indicate that although it can be regenerated, the capacity decreases with each successive regeneration cycle. More work is required on regeneration to improve the lifespan of the zeolite.

In conclusion, simple and quick experiments can be used to screen for potential adsorption applications. This fundamental study introduces a new dimension to the utilisation of naturally occurring material for the treatment of industrial wastewater. These also manifest a possible alternative low cost adsorbent as compared to synthetic materials used in treatment of wastewater. The results obtained in this experimental screening indicate that further investigation of column adsorption and regeneration of Clinoptilolite should be carried out which, thus, allow possible solution for treatment of wastewater in the mining and battery industries.

REFERENCES

Ames, L.L (1960), *Amer. Mineral*., 45, 689

Bailey, S. E., Olin, T.J., Bricka, R. M and Adrian, D.D (1999), *Wat. Res,* 33, 11, 2469

Breck, D.W (1974), *Zeolite Molecular Sieves*., John Wiley and Sons, New York

Brooke (1822), *Edinburgh Phil*. J., 6, 18

Casey, T.J (1997), *Unit Treatment process in Water and Wastewater Engineering*, John Wiley and Sons, New York, 113-114

Chelishchev, N.F., Berinshtein, T. A., Gribanova, N.K and Martynova, N.S (1973), Ion Exchange properties of Clinoptilolite, *Dokl.Akad. Nauk. SSSR,* 210

Choe, J.W., Kim, J.H. and Chung, H.T (1999), *J.Enviromental Science Health*, A34 (7), 1553-1567

Colella, C., Pansini, F., Alfani, M., Canterella, M and Gallfuoco, A (1994), "Selective Water Adsorption from Aqueous Ethanol Containing Vapours by Phillipsite-rich Volcanic Tuffs", *Microporous Matter*, 3, 219

Cooney, E.L., Booker, N.A and Shallcross, D.C (1999), *Separation Science and Technology*, 34 (12), 2307-2327

Couture, R.A (1977), *Chem. Geol*., 19, 113

Cronstedt, A.F (1756), *Akad. Handl. Stockholm*, 17, 120

Dal Bosco, S.M., Jimenez, R.S and Carvalho, W.A (2005), Removal of toxic metals from waste water by Brazilian natural scolecite, *Journal of Colloid and Interface Science*, 281, 242-431

Desborough, G. A (1995), *U.S. Geological Survey (Preliminary report)*, Open file Report, 45-49

Dietz, W. A (1966), J. *Gas Chrom*, 2, 68

Dyer, A (1984), Chemistry *and Industry*, 7, 241

Hein, M., Pflug, H.D. and Henkel, A (1999), *VGB PowerTech,* (3), 61-66

Inglezakis, V.J., Loizidou, M.M and Grigoropoulou, H.P (2004), Ion exchange studies on natural and modified zeolites and the concept of exchange site accessibility, *Journal of Colloid and Interface Sciences*, 275, 570-576

Koon, J.H and Kaufman, W. J (1974), Ammonia removal from municipal wastewaters by ion-exchange. *Journal of Water Pollution Control Federation*, 47, 448-464

Lee, J.D (1991), *Concise Inorganic Chemistry Fourth Edition*, Chapman and Hall, New York

Leppert, D (1990), *Mining Eng*, 42 (6), 604-608

Marcus, B.K. and Cornier, W.E (2001), Zeolite technologies for a greener environment, *Amer. Chem.Soc. Symposium*., 766, 159-173

Marcus, V (1991), Thermodynamics of Solvation of Ions, *J. Chem. Soc. FARADY TRANS.,* 87(18), 2995-2999

Mikhail, K.Y (1981), Radioactive waste treatment using zeolites, Ph.D. Thesis, University of Salford

Moshesh, F, M and Ntlango, X, R (2004), Regeneration of natural zeolite, Fourth year Project, University of the Witwatersrand

Muhammad N., Parr, J., Smith, M.D and Wheatley, A.D (1998), *Sanitation and Water for all*, 24th WEDC Conference, 346-349

Mumpton, F.A (1960), *Amer. Mineral*., 45, 350

Mumpton eds (1978), Natural Zeolites, *Pergamon Press, Oxford*, 135-144

Natural and Synthetic Zeolites (1987), Information Circular 9140, US Department of Interior, *Bureau of Mines*, 3

Ouki, S.K. and Kavannagh. M (1999), *Wat. Sci. Tech.* Vol. 39, No 10-11, 115

Perry, R.H.; Green, D.W. and Maloney, J.O (1997), Perry's Chemical Engineers Handbook, 7th Edition, McGraw-Hill

Rees, L.V.C and Williams, C.J (1964), *J. Chem. Soc. FARADY TRANS*., 60, 1973-1984.

Teo, W.K and Ruthven, D.M (1985), " Adsorption of Water from Aqueous Ethanol Using 3A Molecular Sieves", *Ibid*., 25, 1

Tihmillioglu, F. and Ulku, S (1996), *Separation Science and Technology*, 31, 2855-2865

Townsend, R.P (1984), *Chemistry and Industry*, 7, 246.

Tsitsishvilli, G.M., & Pavliashvilli, V.M (1980), *Izv, Akad* (Nauk. Cruz. SSr.), 6, 188-1891.

Virta, R.L (2000), Zeolites*, U.S Geological Survey Minerals Yearbook*, , 85.1.

Whan, D.A (1981), *Chem. In Britain*, 17, 11.

Yang, H., Ping, Z., Niu, G., Jiang, H and Ling, Y (1999), *Langmuir*, 15, 5382-5388.

Zorpas, A.A and Loizidou, M (1999), " The use of Inorganic Material such as Zeolite for the Uptake of Heavy Metals from Compositing Process", *Hazardous and Industrial Waste.,* 31, 611-620

Appendix A: GC Calibration

Table A1: GC Linearity

Attenuation	Water peak Area	Acetone Peak Area	Area Ratio	Volume (µL)
5	0	0	0	0
	738.7335	5903.9544	7.9920	0.5
	1560.0351	11934.2251	7.6500	1
	2342.3620	18370.0351	7.8425	1.5
	3157.5683	25003.8794	7.9187	2
	4105.6842	32034.5376	7.8025	2.5
	6334.4962	40381.5921	6.3749	3
6	0	0	0	0
	470.8062	3570.9006	7.5846	0.5
	902.9974	6763.0198	7.4895	1
	1362.7067	9819.1918	7.2057	1.5
	1822.1165	12670.1332	6.9535	2
	2421.0673	15457.5271	6.3846	2.5
	3135.5298	20938.2314	6.6777	3
	3777.4032	24418.9562	6.4645	4
7	0	0	0	0
	437.4057	3552.9857	8.1229	2
	788.2278	5464.5693	6.9327	4
	1141.8844	8167.3456	7.1525	6
8	0	0	0	0
	118.7823	1289.6587	10.8573	2
	459.8079	3391.7635	7.3765	4
	993.662	6059.5066	6.0982	6

Peaks Identification and Evaluation

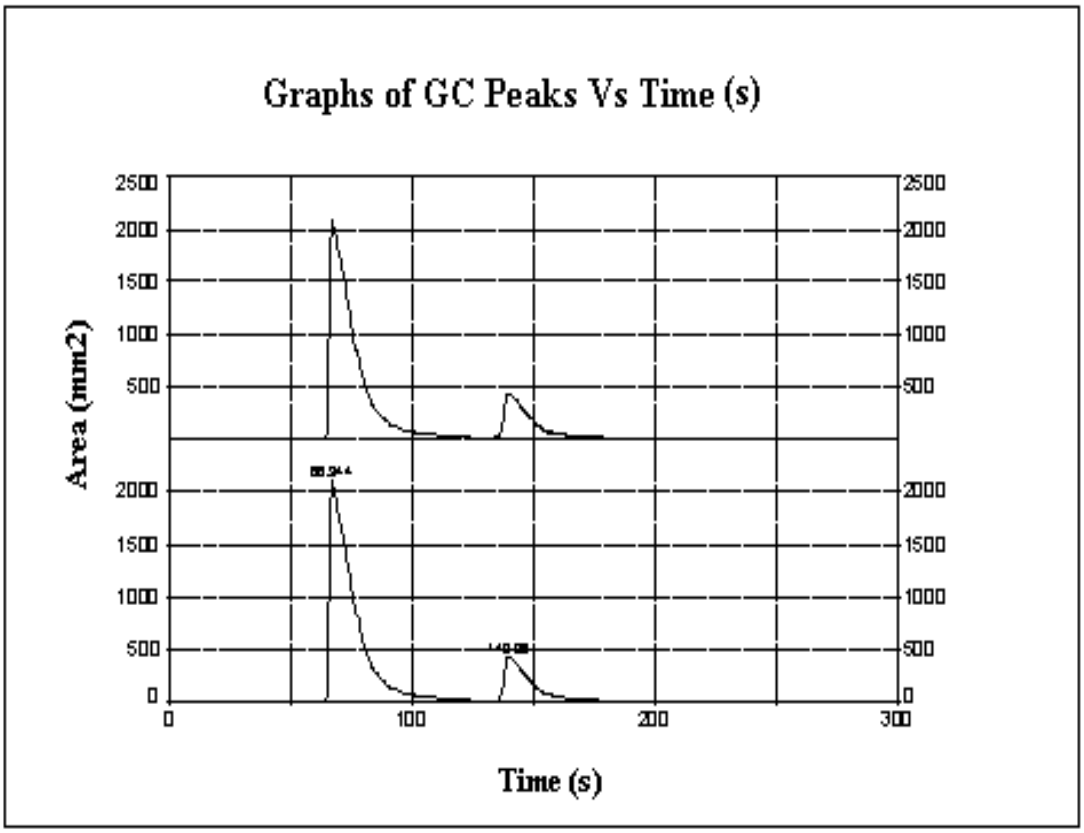

Figure 1A: GC Peaks of Water and Acetone at Column Temperature of 220^0C

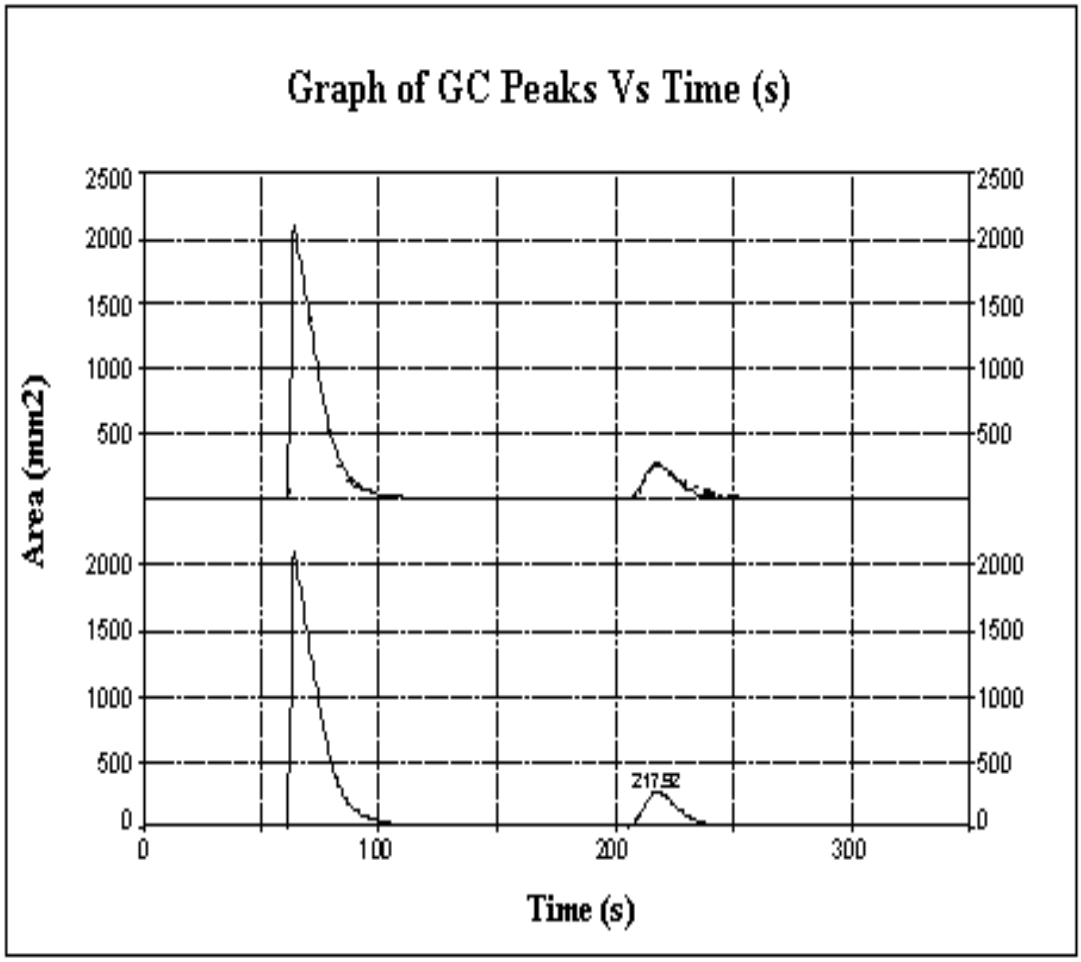

Figure 2A: GC Peaks of Water and Acetone at Column Temperature of 180^0C

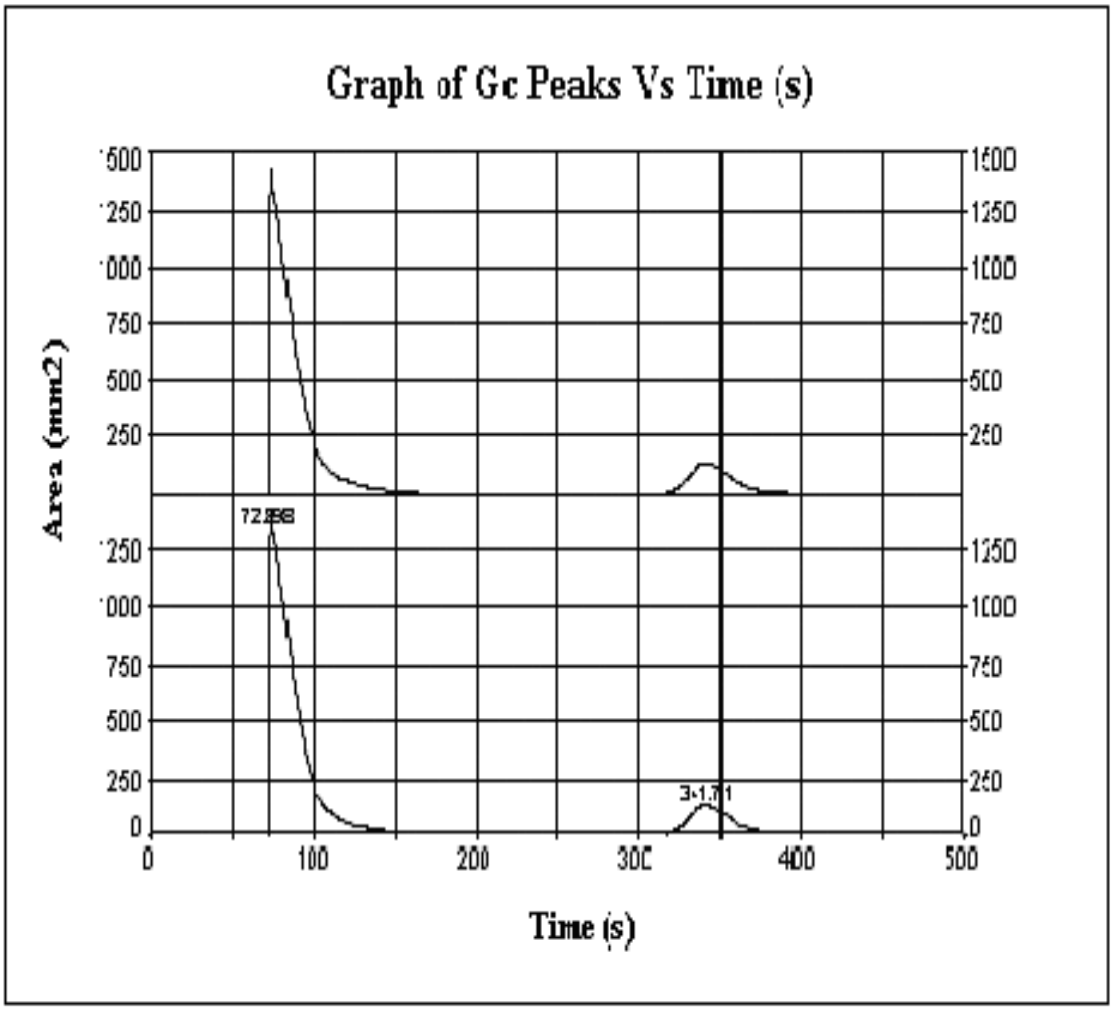

Figure 3A: GC Peaks of Water and Acetone at Column Temperature of 160^0C

Response Factors

Table B1: Acetone-Water Mass Fractions

Sample	Mass of Water (g)	Mass of Acetone (g)	Total Mass	Mass Fraction of Water	Mass Fraction of Acetone
1	1.701	13.410	15.111	0.887	0.113
2	3.682	13.193	16.875	0.782	0.218
3	4.170	6.814	1.984	0.620	0.380
4	5.491	2.120	7.611	0.279	0.721

Table B2: Acetone-Water Area Ratios

Sample	Water Mass Fraction	Acetone Mass Fraction	Water Peak Area	Acetone Peak Area	Area Ratio
1	0.887	0.113	2864.583	19018.131	0.1506
			2775.633	18280.493	0.1518
				Average	**0.1513**
2	0.782	0.218	4970.461	15509.134	0.3205
			4803.318	14803.276	0.3244
				Average	**0.3225**
3	0.620	0.380	10238.312	12762.278	0.8022
			10833.070	13054.692	0.8298
				Average	**0.8160**
4	0.279	0.721	27099.861	8759.003	3.0939
			26672.540	8744.869	3.0501
				Average	**3.0720**

Water and Acetone Response Factor Ratios

The following equations were used to calculate response factor ratio:

$$\text{Mass fraction of A} = \frac{K_A * Peak\ AreaA}{K_A \times Peak\ AreaA + K_B * Peak\ AreaB} \quad \text{……..(B1)}$$

From the above equation the response factor is calculated as follows:

$$\frac{K_B}{K_A} = \left[\frac{1}{Mass\ fraction\ of\ A} - 1\right] * \frac{Peak\ areaA}{Peak\ areaB} \quad \text{…….(B2)}$$

Table B3: Predicted Response Factor Ratios for Water and Acetone

Water Mass Fraction	**Acetone Mass Fraction**	**Water Peak Area**	**Acetone Peak Area**	**Area Ratio**	$\frac{Acetone\ \text{Re}\ sponse}{Water\ \text{Re}\ sponse}$
0.887	0.113	2864.583	19018.131	0.151	1.192
		2775.633	18280.493	0.152	
			Average	**0.151**	
0.782	0.218	4970.461	15509.134	0.321	1.156
		4803.318	14803.276	0.324	
			Average	**0.323**	
0.620	0.380	10238.312	12762.278	0.802	1.333
		10833.070	13054.692	0.830	
			Average	**0.816**	
0.279	0.721	27099.861	8759.003	3.094	1.186
		26672.540	8744.869	3.050	
			Average	**3.072**	**1.217**

Table B4: Standard Deviation of Acetone-Water Response Factor Ratio

Sample	**Ri**	**Ri -** $\overline{R}$	**(Ri -** $\overline{R}$ **)^2**
1	1.192	-0.025	0.001
2	1.156	-0.061	0.004
3	1.333	0.116	0.014
4	1.186	-0.031	0.001
	$\overline{R}$ **= 1.217**		**Sum = 0.019**

$$\text{Standard deviation} = \sqrt{\left(\frac{1}{N-1}\sum(R_i - \bar{R})^2\right)} \quad \ldots\ldots\ldots\ldots\ldots\ldots\ldots\ldots(3)$$

Where R_i individual response factor and $\overline{R}$ mean of the response factors.

Table B5: Ethanol-Water Mass Fractions

Sample	**Mass Of Water (G)**	**Mass Of Ethanol (G)**	**Total Mass**	**Mass Fraction Of Water**	**Mass Fraction Of Ethanol**
1	3.025	9.820	12.845	0.236	0.764
2	2.461	10.052	12.513	0.197	0.803
3	8.542	5.125	13.667	0.625	0.375
4	11.580	3.593	15.173	0.763	0.237

Table B6: Ethanol-Water Area Ratios

Sample	Water Mass Fraction	Ethanol Mass Fraction	Water Peak Area	Ethanol Peak Area	Area Ratio
1	0.236	0.764	2654.607	7803.738	2.940
			2680.661	7958.309	2.969
				Average	**2.954**
2	0.197	0.803	2132.855	7438.951	3.488
			2235.578	7955.910	3.559
				Average	**3.523**
3	0.625	0.375	9351.439	4521.936	0.484
			8283.276	4093.349	0.494
				Average	**0.489**
4	0.763	0.237	9945.120	2834.514	0.285
			9774.547	2864.003	0.293
				Average	**0.289**

Table B7: Predicted Response Factor Ratio for Ethanol and Water

Water Mass Fraction	Ethanol Mass Fraction	Water Peak Area	Ethanol Peak Area	Area Ratio	$\frac{Ethanol\ \mathrm{Re}sponse}{Water\ \mathrm{Re}sponse}$
0.236	0.764	2654.607	7803.738	2.940	**1.099**
		2680.661	7958.309	2.969	
			Average	**2.954**	
0.197	0.803	2132.855	7438.951	3.488	**1.159**
		2235.578	7955.910	3.559	
			Average	**3.523**	
0.625	0.375	9351.439	4521.936	0.484	**1.228**
		8283.276	4093.349	0.494	
			Average	**0.489**	
0.763	0.237	9945.120	2834.514	0.285	**1.074**
		9774.547	2864.003	0.293	
			Average	**0.289**	

Table B8: Standard Deviation of Ethanol -Water Response Factor Ratio

Sample	**Ri**	**Ri -** $\overline{R}$	**(Ri -** $\overline{R}$ **)^2**
1	1.099	-0.041	**0.002**
2	1.159	0.019	**0.001**
3	1.228	0.088	**0.008**
4	1.074	-0.066	**0.004**
	$\overline{R}$ **= 1.140**		**Sum = 0.015**

Appendix C: GC Errors

Table C1: High Ethanol Concentration Reproducibility Error

Ethanol Mass Fraction (Xi)	Water Peak Area	Ethanol Peak Area	Area Ratio	GC Predicted Mass Fraction (Ri)	Ri - $\overline{R}$	(Ri - $\overline{R}$)^2
0.86	3174.46	18600.5	0.169	0.869	0.002	**4.319*10^{-6}**
	3127.03	17940.7	0.1743	0.867	-0.001	**1.059*10^{-7}**
	3661.12	20990.8	0.1744	0.867	-0.001	**1.623*10^{-7}**
	2730.37	15780.0	0.1730	0.868	-0.001	**2.641*10^{-7}**
	2960.36	16759.9	0.1763	0.865	-0.002	**3.474*10^{-6}**
			($\overline{R}$)	**0.868**		**8.325*10^{-6}**

Table C2: Low Ethanol Concentration Reproducibility Error

Ethanol Mass Fraction	Water Peak Area	Ethanol Peak Area	Area Ratio	Predicted Mass Fraction	Ri - $\overline{R}$	(Ri - $\overline{R}$)^2
0.08	9195.02	719.93	12.772	0.082	0.002	**5.447*10^{-6}**
	8895.64	623.82	14.259	0.074	-0.006	**3.118*10^{-5}**
	7993.54	609.67	13.112	0.080	0.001	**1.471*10^{-7}**
	9535.86	736.89	12.941	0.081	0.001	**1.830*10^{-6}**
	9800.57	758.99	12.913	0.081	0.002	**2.292*10^{-6}**
				($\overline{R}$)=0.079		**4.090*10^{-5}**

Table C3: Low Acetone Concentration Reproducibility Error

Acetone Mass Fraction	**Water Peak Area**	**Acetone Peak Area**	**Area Ratio**	**Predicted Mass Fraction**	**Ri - $\overline{R}$**	**(Ri - $\overline{R}$)^2**
0.087	64941.3	5018.2	12.941	0.0859	-0.0005	**$2.138*10^{-7}$**
	64053.5	4920.37	13.018	0.0855	-0.0009	**$8.583*10^{-7}$**
	67486.2	5307.99	12.714	0.0873	0.0009	**$8.804*10^{-7}$**
	66908.9	5258.35	12.724	0.0872	0.0009	**$7.642*10^{-7}$**
	66582	5147.52	12.935	0.0860	-0.0004	**$1.795*10^{-7}$**
				($\overline{R}$)=0.0864		**=$2.896*10^{-6}$**

Table C4: High Acetone Concentration Reproducibility Error

Acetone Mass Fraction	**Water Peak Area**	**Ethanol Peak Area**	**Area Ratio**	**Predicted Mass Fraction**	**Ri - $\overline{R}$ i**	**(Ri - $\overline{R}$)^2**
0.9	2272	16760.7	0.136	0.899	0.00478	**$2.288*10^{-5}$**
	2171	15078.2	0.144	0.894	-0.00079	**$6.246*10^{-7}$**
	2024.8	14191.6	0.143	0.895	0	**0**
	1906.3	13218.1	0.144	0.894	0.00095	**$8.941*10^{-7}$**
	1998	13542.9	0.148	0.892	-0.00312	**$9.712*10^{-6}$**
				($\overline{R}$)=0.895		**$3.411*10^{-5}$**

Experimental Results

Table D1: Ethanol Mass Fractions for Varying Masses of Zeolite

Time (Hrs)	Ethanol Mass Fraction	Ethanol Mass Fraction	Ethanol Mass Fraction	Ethanol Mass Fraction
	10g Zeolite	**20g Zeolite**	**30g Zeolite**	**50g Zeolite**
0	0.0671	0.0671	0.0671	0.0671
6	0.0680	0.0623	0.0533	0.0603
12	0.0656	0.0626	0.0670	0.0575
20	0.0580	0.0637	0.0635	0.0635
28	0.0679	0.0670	0.0539	0.0582
36	0.0679	0.0606	0.0499	0.0644
44	0.0662	0.0622	0.0604	0.0559
52	0.0683	0.0575	0.0656	0.0600
60	0.0608	0.0624	0.0605	0.0597
70	0.0561	0.0547	0.0587	0.0554
100	0.0625	0.0600	0.0630	0.0614

Table D2: Ethanol Mass Fraction from 85.8% for Varying Masses of Zeolite

Time (Hrs)	Ethanol Mass Fraction	Ethanol Mass Fraction	Ethanol Mass Fraction	Ethanol Mass Fraction
	10g Zeolite	**10g Zeolite**	**20g Zeolite**	**50g Zeolite**
0	0.8587	0.8587	0.8587	0.8587
6	0.8595	0.8601	0.8605	0.8597
12	0.8591	0.8594	0.8596	0.8592
20	0.8592	0.8607	0.8613	0.8622
28	0.8592	0.8605	0.8615	0.8621
34	0.8602	0.8607	0.8610	0.8633
44	0.8605	0.8612	0.8621	0.8626
53	0.8607	0.8617	0.8617	0.8624

Density of Aqueous Ethanol Solution

The density of aqueous ethanol solution was calculated using the following equation obtained in Perry et al, (1997).

$$\text{Density of solution} = \text{mass\%}\ (-0.2574) + 1.0498 \quad \text{(D3)}$$

The mass percentage of ethanol used to calculate the density of aqueous ethanol solution is obtained from Table D2 (appendix)

Table D3: Density of Aqueous Ethanol Solution

Time (Hrs)	Density of Solution for 10g Zeolite	Density of Solution for 20g Zeolite	Density of Solution for 30g Zeolite	Density of Solution for 50g Zeolite
0	0.8288	0.8288	0.8288	0.8288
6	0.8286	0.8284	0.8283	0.8285
12	0.8287	0.8286	0.8285	0.8286
20	0.8286	0.8283	0.8281	0.8279
28	0.8286	0.8283	0.8281	0.8279
34	0.8284	0.8283	0.8282	0.8276
44	0.8283	0.8281	0.8279	0.8278
53	0.8283	0.8280	0.8280	0.8278

Table D4: Mass of Water in Solution

Mass of water for 100mL of solution = density of aqueous solution* volume* mass%

Mass of Water in Solution (G)				Volume of Solution (Ml)
10g Zeolite	**20g Zeolite**	**30g Zeolite**	**50g Zeolite**	
11.708	11.708	11.708	11.708	100
11.641	11.592	11.553	11.622	100
11.441	11.417	11.398	11.432	98
11.201	11.080	11.026	11.949	96
10.967	10.860	10.782	10.734	94
10.657	10.614	10.594	10.407	92
10.398	10.344	10.278	10.234	90
10.158	10.079	10.076	10.022	88

Mass of Water on Zeolite

Mass of Water adsorbed on the zeolite was calculated as follows:

$$M_A = M_o(l) - M_A(t) - 2 * \sum^{t-1} MAsamplecollected$$

Where M_A =mass of water on the zeolite, $M_0(l)$ is mass of water in solution at t = 0, Mass of water in solution at time t, $\sum^{t-1} M_A samplecollected$ (mass concentration of samples collected) and 2 represent the mL of sample.

Table D5: Mass of Water on Zeolite

Time (Hrs)	**Mass of Water on Zeolite**			
	10g Zeolite	**20g Zeolite**	**30g Zeolite**	**50g Zeolite**
0	0	0	0	0
6	0.068	0.116	0.155	0.087
12	0.035	0.059	0.079	0.044
20	0.041	0.164	0.218	0.294
28	0.042	0.153	0.232	0.281
34	0.118	0.167	0.191	0.379
44	0.146	0.207	0.278	0.326
53	0.158	0.242	0.251	0.311

Mass of Water on Zeolite Per Gram of Zeolite

Mass of Water on Zeolite per g of Zeolite			
10	20	30	50
0	0	0	0
0.0068	0.0058	0.0052	0.0017
0.0035	0.0030	0.0026	0.0009
0.0041	0.0082	0.0073	0.0059
0.0042	0.0076	0.0077	0.0056
0.0118	0.0084	0.0064	0.0076
0.0146	0.0103	0.0093	0.0065
0.0158	0.0121	0.0084	0.0062

Table D7: Changes in Acetone Mass Fraction from Initial Concentration of 8.5% for Varying Masses of Zeolite

Time (Hrs)	Acetone Mass Fraction	Acetone Mass Fraction	Acetone Mass Fraction	Acetone Mass Fraction
	10g Zeolite	20g Zeolite	30g Zeolite	50g
0	0.0851	0.0851	0.0851	0.0851
6	0.0736	0.0685	0.0386	0.0687
12	0.0775	0.0509	0.0747	0.0627
20	0.0796	0.0786	0.0611	0.0775
28	0.0635	0.0592	0.0692	0.0715
36	0.0786	0.0515	0.0640	0.0628
44	0.0736	0.0516	0.0547	0.0673
52	0.0785	0.0691	0.0619	0.0704
60	0.0777	0.0474	0.0563	0.0715
70	0.0784	0.0593	0.0757	0.0665

Table D8: Changes in Acetone Mass Fraction from Initial Concentration of 89.5% for Varying Masses of Zeolite

Time (Hrs)	Acetone Mass Fraction	Acetone Mass Fraction	Acetone Mass Fraction	Acetone Mass Fraction
	10g Zeolite	20g Zeolite	30g Zeolite	50g Zeolite
0	0.8952	0.8952	0.8952	0.8952
6	0.8892	0.8828	0.8750	0.8670
12	0.8792	0.8774	0.8765	0.8777
20	0.8870	0.8773	0.8774	0.8740
28	0.8811	0.8796	0.8748	0.8657
34	0.8859	0.8812	0.8757	0.8744
44	0.8826	0.8789	0.8742	0.8671
53	0.8798	0.8793	0.8767	0.8689

Density of Aqueous Acetone Solution

The density of solution was calculated using the following equation from Perry (1997)

$$d = d_w + Ap_s + Bp_s^2 + Cp_s^3 \quad \text{.....(D9)}$$

For acetone: A = -0.001171

B = -0.00000904

C = -0.0000000056

d_w = density of water at 25^0C = 0.997045 mg/L

d = density of aqueous acetone solution

Table D9: Density of Aqueous Acetone Solution

Time (Hrs)	Density of Solution for 10g Zeolite	Density of Solution for 20g Zeolite	Density of Solution for 30g Zeolite	Density of Solution for 50g Zeolite
0	0.995989	0.995989	0.995989	0.995989
6	0.995997	0.996004	0.996013	0.996023
12	0.996009	0.996011	0.996012	0.99601
20	0.995999	0.996011	0.996011	0.996015
28	0.996006	0.996008	0.996014	0.996025
34	0.996001	0.996006	0.996013	0.996014
44	0.996004	0.996009	0.996014	0.996023
53	0.996008	0.996008	0.996011	0.996021

Mass of Acetone in Solution

Mass of acetone in solution = density of aqueous solution* volume* mass% of acetone

Table D10: Mass of Acetone in Solution

Time (Hrs)	10g Zeolite	20g Zeolite	30g Zeolite	50g Zeolite	Volume of Solution (Ml)
0	89.16586	89.16586	89.16586	89.16586	100
6	88.56408	87.92852	87.14907	86.35886	100
12	85.81332	85.64659	85.55796	85.67243	98
20	84.81188	83.88436	83.89754	83.56694	96
28	82.49427	82.35271	81.90247	81.04975	94
34	81.17313	80.74828	80.2397	80.12683	92
44	79.11526	78.7815	78.36035	77.73143	90
53	77.11004	77.06546	76.83911	76.15708	88

Mass Of Acetone On Zeolite

Mass of acetone adsorbed on the zeolite was calculated as follows:

$$M_A = M_o(l) - M_A(t) - 2 * \sum^{t-1} MAsamplecollected \quad \text{.....(D11)}$$

Where M_A =mass of acetone on the zeolite, $M_0(l)$ is mass of acetone in solution at t = 0, Mass of acetone in solution at time t, $\sum^{t-1} M_A samplecollected$ (mass concentration of samples collected) and 2 represent the mL of sample.

Table D11: Mass of Acetone on Zeolite

	Mass of Acetone on Zeolite			
Time (Hrs)	**10g Zeolite**	**20g Zeolite**	**30g Zeolite**	**50g Zeolite**
0	0	0	0	0
6	0.601786	1.237338	2.016796	2.807005
12	1.581258	1.760703	1.864926	1.766252
20	0.831407	1.775042	1.779264	2.123327
28	1.382103	1.559106	2.026465	2.899542
34	0.948049	1.411343	1.94663	2.098003
44	1.241289	1.622727	2.081634	2.751508
53	1.488392	1.588072	1.861534	2.598492

Table D12: Mass of Acetone on Zeolite Per Gram of Zeolite

Mass of Acetone on Zeolite Per Gram of Zeolite			
10g Zeolite	**20g Zeolite**	**30g Zeolite**	**50g Zeolite**
0	0	0	0
0.115288	0.082867	0.154627	0.032799
0.092009	0.175965	0.039489	0.047226
0.087152	0.048024	0.088122	0.021472
0.254167	0.146929	0.066932	0.035693
0.128271	0.188148	0.087272	0.054512
0.188702	0.193163	0.119506	0.049076
0.160175	0.121498	0.10201	0.046171

Appendix E: Zn^{2+} Adsorption Results

Table E1: Summary of the Adsorption Experimental Results for Zn^{2+}

Time (Hrs)	Zn^{2+} (mg/L)	Zn^{2+} (mg/L)	Zn^{2+} (mg/L)	Zn^{2+} (mg/L)	Volume
	10g Zeolite	20g Zeolite	30g Zeolite	50g Zeolite	(mL)
0	45	45	45	45	100
1	39.7	32.5	26.3	20.1	100
2	35.3	29.9	24.7	18.2	98
3	35	29	24.5	18.1	96
4	35	29	24.4	18	94
5	35	29	24	18	92
6	35	29	24	18	90
7	35	29	24	18	88
8	35	29	24	18	86

Table E2: Mg of Zn^{2+} in Solution

Volume	**Zn^{2+}**	**Zn^{2+}**	**Zn^{2+}**	**Zn^{2+}**
	10g Zeolite	**20g Zeolite**	**30g Zeolite**	**50g Zeolite**
100	4.5	4.5	4.5	4.5
100	3.97	3.25	2.63	2.01
98	3.4594	2.9302	2.4206	1.7836
96	3.36	2.784	2.352	1.7376
94	3.29	2.726	2.2936	1.692
92	3.22	2.668	2.208	1.656
90	3.15	2.61	2.16	1.62
88	3.08	2.552	2.112	1.584
86	3.01	2.494	2.064	1.548

Table E3: Mg of Zn^{2+} on Zeolite

Volume	**Zn^{2+}**	**Zn^{2+}**	**Zn^{2+}**	**Zn^{2+}**
	10g Zeolite	**20g Zeolite**	**30g Zeolite**	**50g Zeolite**
100	0	0	0	0
100	0.53	1.25	1.85	2.44
98	0.96	1.51	2.01	2.63
96	0.99	1.59	2.03	2.65
94	0.99	1.59	2.04	2.65
92	0.99	1.59	2.07	2.65
90	0.99	1.59	2.07	2.65
88	0.99	1.59	2.07	2.65
86	0.99	1.59	2.07	2.65

Table E4: Mg of Zn^{2+} Per Gram of Zeolite

Time	**10g Zeolite**	**20g Zeolite**	**30g Zeolite**	**50g Zeolite**
0	0	0	0	0
1	16.21	19.12	18.86	14.93
2	29.40	23.02	20.46	16.07
3	30.28	24.34	20.66	16.13
4	30.28	24.34	20.75	16.18
5	30.28	24.34	21.13	16.18
6	30.28	24.34	21.13	16.18
7	30.28	24.34	21.13	16.18
8	30.28	24.34	21.13	16.18
9	30.28	24.34	21.13	1.618

Appendix F: Ni^{2+} Adsorption Results

Table F1: Summary of the Adsorption Experimental Results for Ni^{2+}

Time (Hrs)	Ni^{2+}	Ni^{2+}	Ni^{2+}	Ni^{2+}	Volume (mL)
	10g Zeolite	**20g Zeolite**	**30g Zeolite**	**50g Zeolite**	
0	45.00	45.00	45.00	45.00	100
1	42.01	38.24	35.32	29.71	100
2	39.50	34.23	30.00	25.13	98
3	38.23	32.71	29.22	23.42	96
4	37.84	33.01	28.94	23.32	94
5	38.00	32.85	28.92	23.27	92
6	37.75	32.90	28.51	23.11	90
7	37.61	33.13	28.45	23.26	88
8	37.72	33.11	28.43	23.34	86

Table F2: Mg of Ni^{2+} in Solution

Time (Hrs)	Ni^{2+}	Ni^{2+}	Ni^{2+}	Ni^{2+}	Volume (mL)
	10g Zeolite	**20g Zeolite**	**30g Zeolite**	**50g Zeolite**	
0	4.50	4.50	4.50	4.50	100
1	4.20	3.82	3.53	2.97	100
2	3.95	3.42	3.00	2.51	98
3	3.82	3.27	2.92	2.34	96
4	3.78	3.30	2.89	2.33	94
5	3.80	3.29	2.89	2.33	92
6	3.78	3.29	2.85	2.31	90
7	3.76	3.31	2.85	2.33	88
8	3.77	3.31	2.84	2.33	86

Table F3: Mg of Ni^{2+} on Zeolite

Time (Hrs)	**Ni^{2+}**	**Ni^{2+}**	**Ni^{2+}**	**Ni^{2+}**	**Volume (Ml)**
	10g Zeolite	**20g Zeolite**	**30g Zeolite**	**50g Zeolite**	
0	0	0	0	0	100
1	0.30	0.68	0.97	1.53	100
2	0.55	1.07	1.49	1.99	98
3	0.69	1.22	1.57	2.14	96
4	0.71	1.19	1.59	2.15	94
5	0.69	1.20	1.59	2.16	92
6	0.72	1.19	1.63	2.17	90
7	0.73	1.18	1.64	2.16	88
8	0.72	1.18	1.64	2.15	86

Table F4: Mg of Ni^{2+} Per Gram of Zeolite

Time (Hrs)	**Ni^{2+}**	**Ni^{2+}**	**Ni^{2+}**	**Ni^{2+}**	**Volume (mL)**
	10g Zeolite	**20g Zeolite**	**30g Zeolite**	**50g Zeolite**	
0	0	0	0	0	100
1	10.22	11.58	11.02	10.43	100
2	18.57	18.62	16.92	13.57	98
3	23.48	20.72	17.78	14.61	96
4	24.12	20.73	18.10	14.67	94
5	24.39	20.75	18.22	14.74	92
6	24.41	20.74	18.56	14.91	90
7	24.41	20.75	18.57	14.99	88
8	24.41	20.75	18.57	14.99	86

Appendix G: Pb^{2+} Adsorption Results

Table G1: Summary of the Adsorption Experimental Results for Pb^{2+}

Time (Hrs)	Pb^{2+} 10g Zeolite	Pb^{2+} 20g Zeolite	Pb^{2+} 30g Zeolite	Pb^{2+} 50g Zeolite	Volume (Ml)
0	45.00	45.00	45.00	45.00	100
1	22.31	19.23	15.82	2.54	100
2	11.52	7.45	5.95	0.98	98
3	9.00	5.22	4.21	0.11	96
4	8.83	4.15	3.17	0.14	94
5	8.37	3.36	2.20	0.18	92
6	8.25	3.41	1.63	0.22	90
7	8.29	2.93	1.59	0.15	88
8	8.33	3.10	1.55	0	86

Table G2: Mg of Pb^{2+} in Solution

Time (Hrs)	**Pb^{2+}**	**Pb^{2+}**	**Pb^{2+}**	**Pb^{2+}**	**Volume (Ml)**
	10g Zeolite	**20g Zeolite**	**30g Zeolite**	**50g Zeolite**	
0	4.50	4.50	4.50	4.50	100
1	2.23	1.92	1.58	0.25	100
2	1.13	0.67	0.59	0.10	98
3	0.86	0.50	0.42	0.01	96
4	0.76	0.42	0.32	0.01	94
5	0.74	0.38	0.22	0.02	92
6	0.73	0.34	0.16	0.02	90
7	0.74	0.29	0.13	0.02	88
8	0.74	0.31	0.13	0	86

Table G3: Mg of Pb^{2+} on Zeolite

Time (Hrs)	Pb^{2+}	Pb^{2+}	Pb^{2+}	Pb^{2+}	Volume (Ml)
	10g Zeolite	20g Zeolite	30g Zeolite	50g Zeolite	
0	0	0	0	0	100
1	2.3	2.60	3.01	4.25	100
2	3.33	3.78	3.89	4.41	98
3	3.57	3.95	4.064.16	4.48	96
4	3.59	4.05	4.24	4.48	94
5	3.63	4.13	4.29	4.48	92
6	3.64	4.12	4.30	4.47	90
7	3.64	4.16	4.30	4.49	88
8	3.63	4.15	4.29	4.49	86

Table G4: Mg of Pb^{2+} Per Gram of Zeolite

Time (Hrs)	**Pb^{2+}**	**Pb^{2+}**	**Pb^{2+}**	**Pb^{2+}**	**Volume (Ml)**
	10g Zeolite	**20g Zeolite**	**30g Zeolite**	**50g Zeolite**	
0	0.00	0.00	0.00	0.00	100
1	22.20	12.55	9.65	8.20	100
2	32.13	18.22	12.52	8.51	98
3	34.45	19.06	13.05	8.65	96
4	34.63	19.56	13.38	8.66	94
5	35.08	19.91	13.65	8.66	92
6	35.16	19.87	13.82	8.64	90
7	35.09	20.08	13.85	8.65	88
8	35.09	20.08	13.85	8.65	86

Appendix H: Metal Ions Adsorption Isotherms Results

Table H1: Metal Ions Langmuir Adsorption Isotherms Results

Zn^{2+}		Ni^{2+}		Pb^{2+}	
Ce (mg/L)	**Ce/Qe**	**Ce (mg/L)**	**Ce/Qe**	**Ce (mg/L)**	**Ce/Qe**
0	0	0	0	0	0
18	1.618	23.3	1.468	1.55	1.383
24	2.113	28.43	1.859	3.00	2.004
29	2.434	33.00	2.024	8.33	3.505
23	3.029	37.70	2.442	8.33	3.505

Table H2: Metal Ions Freundlich Adsorption Isotherms Results

Zn^{2+}		Ni^{2+}		Pb^{2+}	
Ln(Ce)	**Ln(Qe)**	**Ln(Ce)**	**Ln(Qe)**	**Ln(Ce)**	**Ln(Qe)**
0.000	0.000	0.000	0.000	0.000	0.000
3.148	2.765	2.890	2.409	0.438	0.114
3.347	2.728	3.178	2.430	1.099	0.403
3.497	2.791	3.367	2.478	2.120	0.866
3.630	2.737	3.555	2.447	2.120	0.866

Table H3: Metal Ions Langmuir Isotherms Results

	Linear equation	Correlation Coefficient r2	Langmuir Constant
Zn^{2+}	y= 0.086x + 0.025	0.998	11.69
Ni^{2+}	y= 0.064x + 0.003	0.997	15.8
Pb^{2+}	y= 0.412x + 0.318	0.926	2.43

Table H4: Metal Ions Freundlich Isotherms Results

	Linear Equation	Correlation Coefficient r2	Freundlich Constant
Zn^{2+}	y= 0.733x + 0.049	0.977	1.05
Ni^{2+}	y= 0.797x + 0.030	0.986	1.03
Pb^{2+}	y= 0.417x - 0.036	0.993	0.96

Appendix I: Loading on Clinoptilolite

This appendix contains the experimental results of a 4th year laboratory project carried out by Moshesh and Ntlango (2004) as a result of the work undertaken in this study and the work carried out by the 2001 4th-year students, Lieshout and Vassiloudos (2001), who I co-supervised. I did not supervise Moshesh and Ntlango (2004), as I had already begun working in industry and was registered as a part-time student.

Table I1 and Table I2 are representations of the experimental data generated in the loading of iron ions and copper onto Clinoptilolite, respectively. The table shows the change in concentration with time.

Table I1: Experimental Data for Loading of Fe^{2+} to Clinoptilolite, from a 50ppm Solution.

Time (Hrs)	10g	30g	50g
1	42.8	39.6	37.4
2.5	45.1	37.9	35.1
4	41.2	35.8	32.9
5	41.4	33.1	29.3
6	41.6	34.2	31
7	38	31.1	27.5
25	36.3	29.5	23
26.5	37.7	27.8	20.1
27.5	34.5	27.7	20.6

Table I2: Experimental Data for Loading of Cu^{2+} to Clinoptilolite from a 50ppm Solution

Time (Hrs)	**10g**	**20g**	**30g**	**40g**	**50g**
	10	20	30	40	50
0	50	50	50	49.933	49.933
1	47.9	45.3	44.6	40.7	37.3
2	8.4	42.8	40.6	36.4	32.9
3	46.2	41.6	37.1	33.7	29.5
3.9167	45.4	39	33.5	31.2	31.3
5	43.6	38.3	32	29	23.8
6.5	40.6	33.1	29.2	26.8	22.6
8.1667	40.4	31.9	27.5	22.9	18.8
9.5833	41.7	31.8	27.7	23.6	19.5
10.25	24.2	20.6	14.5	10.6	9
24.5	38.6	29.8	22.7	21.3	17.7
25.5	37.5	28.7	24.2	20.4	17

Table I3 and I4 represent the experimental data for the loading of Cu^{2+} and Fe^{2+} onto the zeolite and the regenerated zeolite.

Table I3: Experimental Data for Loading of Cu^{2+} onto the Zeolite and Regeneration of Cu^{2+} Loaded Zeolite.

Loading of Cu^{2+} onto the Zeolite: Experimental Results			
Mass of zeolite (g)	**10**	**30**	**50**
Concentration at equilibrium (ppm)	31.1	18.9	17.4
Mass loaded (mg)	2.835	4.665	4.89
Regeneration of Cu^{2+} Loaded Zeolite Experimental Results			
Time (Hrs)	**Concentration in ppm**		
0	0	0	0
19.5	10	10.8	5.8
26	11	14.4	12.4
67.5	12.5	18.8	16.2
103.5	12	21.3	18
122.5	12.7	19.1	17.4
120.5	12.8	19.8	28
Loading of Cu^{2+} onto Regenerated Zeolite: Experimental Results			
Mass of Zeolite (g)	**10**	**30**	**50**
Concentration at equilibrium (ppm)	34.3	20.7	19.8
Mass loaded (mg)	1.55	2.97	3.13

Table I4: Experimental Data for the Loading Fe^{2+} onto the Zeolite and Regeneration of Fe^{2+} Loaded Zeolite**.**

Loading of Fe^{2+} onto Virgin Zeolite: Experimental Results			
Mass of Zeolite (g)	**10**	**30**	**50**
Concentration at equilibrium (ppm)	24.3	15.6	7.4
Mass loaded (mg)/g zeolite	4.665	2.835	2.61
Regeneration of Fe^{2+} Loaded Zeolite: Experimental Results			
Time (Hrs)	**Concentration in ppm**		
0	0	0	0
19.5	*7.6*	*7.9*	*4.5*
26	13	15.2	9.4
43.5	15.5	17.8	13.2
55.5	16.2	22.4	15
98.5	17.7	23.1	16.4
120.5	17.8	23.8	18.6
146.5	18.1	24.2	19
Loading of Fe^{2+} onto Regenerated Zeolite: Experimental Results			
Mass of Zeolite (g)	**10**	**30**	**50**
Concentration at equilibrium (ppm)	29.3	17.5	13.7
Mass loaded (mg)	2.55	1.82	1.056